

It's TIME: Towards the Next Generation of Time Series Forecasting Benchmarks

Zhongzheng Qiao¹ Sheng Pan² Anni Wang³ Viktoriya Zhukova³ Yong Liu⁴ Xudong Jiang¹ Qingsong Wen⁵
Mingsheng Long⁴ Ming Jin² Chenghao Liu³

Abstract

Time series foundation models (TSFMs) are revolutionizing the forecasting landscape from specific dataset modeling to generalizable task evaluation. However, we contend that existing benchmarks exhibit common limitations in four dimensions: constrained data composition dominated by reused legacy sources, compromised data integrity lacking rigorous quality assurance, misaligned task formulations detached from real-world contexts, and rigid analysis perspectives that obscure generalizable insights. To bridge these gaps, we introduce TIME, a next-generation task-centric benchmark comprising 50 fresh datasets and 98 forecasting tasks, tailored for strict zero-shot TSFM evaluation free from data leakage. Integrating large language models and human expertise, we establish a rigorous human-in-the-loop benchmark construction pipeline to ensure high data integrity and redefine task formulation by aligning forecasting configurations with real-world operational requirements and variate predictability. Furthermore, we propose a novel pattern-level evaluation perspective that moves beyond traditional dataset-level evaluations based on static meta labels. By leveraging structural time series features to characterize intrinsic temporal properties, this approach offers generalizable insights into model capabilities across diverse patterns. We evaluate 12 representative TSFMs and establish a multi-granular leaderboard to facilitate in-depth analysis and visualized inspection. The leaderboard is available at <https://huggingface.co/spaces/Real-TSF/TIME-leaderboard>.

¹Nanyang Technological University ²Griffith University
³DataDog ⁴Tsinghua University ⁵Squirrel Ai Learning. Correspondence to: Zhongzheng Qiao <qiao00020@e.ntu.edu.sg>, Ming Jin <mingjinedu@gmail.com>, Chenghao Liu <chenghao.liu@datadoghq.com>.

Preprint. February 13, 2026.

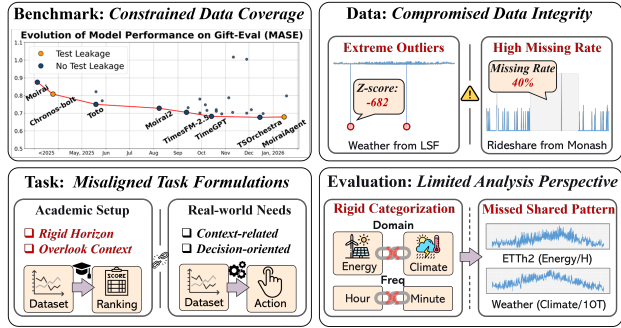


Figure 1. Common bottlenecks in prevalent TSF benchmarks.

1. Introduction

Time series foundation models (TSFMs) have reshaped the evaluation landscape of time series forecasting (TSF), shifting the dominant paradigm from a *dataset-centric regime*, where models are trained and assessed within individual datasets, to a *task-centric regime* that emphasizes zero-shot generalization across forecasting tasks. This paradigm shift has also exposed fundamental insufficiencies in widely adopted TSF benchmarks (Zhou et al., 2021; Wu et al., 2021). Recent studies (Hewamalage et al., 2023; Bergmeir, 2024; Brigato et al., 2026) have revealed critical limitations, including questionable data forecastability and misaligned evaluation protocol misalignment, whose effects can be obscured in task-centric benchmarking settings that evaluate models across a large number of heterogeneous datasets. In response, recent years have witnessed intensified efforts (Aksu et al., 2024; Cohen et al., 2025; Shchur et al., 2025) to develop more advanced TSF benchmarks that aim to move beyond traditional dataset-centric evaluation.

While these initiatives have introduced valuable refinements, a central challenge remains: *how can TSF benchmarking be fundamentally reoriented toward the task-centric evaluation paradigm required by TSFMs?* We argue that addressing this challenge requires confronting a set of persistent structural limitations in existing TSF benchmarks. As shown in Figure 1, we identify four critical dimensions: **(1) Legacy-Constrained Data Coverage.** The data composition of modern benchmarks remains heavily constrained by *legacy* datasets (see Figure 2). This limited coverage is reflected in plateaued performance where model improvements on established benchmarks have visibly slowed down

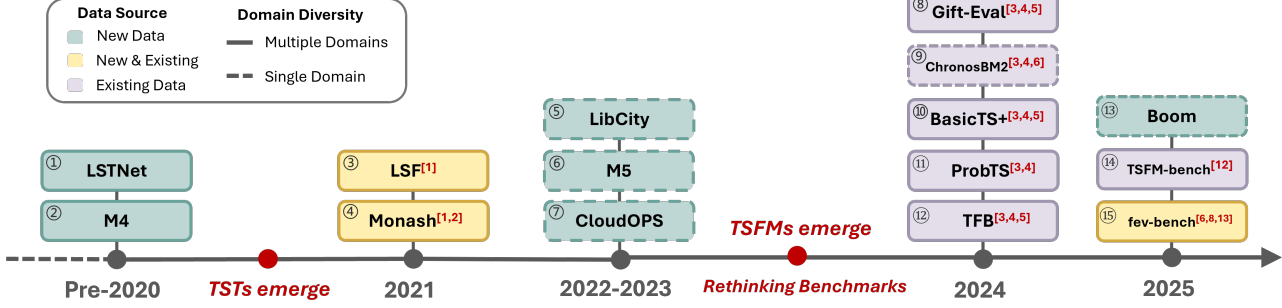


Figure 2. Timeline of time series forecasting (TSF) benchmarks. Each block represents a TSF benchmark, where color indicates the **data source** and outline style represents the **domain diversity**. Superscripts mark the prior benchmarks whose datasets are reused in each work. Major milestones and transitions in the field are highlighted in red along the timeline. **TST** denotes Time Series Transformer.

(e.g. Gift-Eval shown in Figure 1), while simultaneously amplifying the growing risk of benchmark contamination from data leakage. **(2) Compromised Data Integrity.** Rigorous quality assurance is often overlooked in dataset curation, including poor-quality variates with extreme outliers or excessive missing values (Wu et al., 2021; Godahewa et al., 2021). **(3) Misaligned Task Formulations.** Rigid, mechanical setups detach forecasting requirements from real-world contexts (Bergmeir, 2024), ignoring predictable horizons and variate predictability. **(4) Limited Analysis Perspective.** Current evaluations categorize datasets by rigid meta labels (Aksu et al., 2024; Qiu et al., 2024) and aggregate dataset-level results as the performance indicator on the specific domain or frequency. While offering macro-level ranking, this perspective ignores that variates across domains/frequencies often exhibit similar temporal characteristics, resulting in limited insight into why a model performs well and offer weak guidance for selecting models in specific application scenarios.

Moreover, unlike modalities with intuitive performance proxies (e.g., classification accuracy in NLP), time-series error metrics are inherently abstract and do not directly reflect the structural fidelity or operational usefulness of predictions. For example, Figure 14 illustrates a prediction by TimesFM 2.5 (Das et al., 2024) on a test window. Although the metric appears favorable (MASE=0.662, MAE=1.12), the forecast fails to capture the distinct spike structure of the series. Thus, over-reliance on such numerical rankings risks decoupling benchmark conclusions from practical decision-making in real-world temporal settings.

To bridge these gaps, we introduce TIME, a next-generation task-centric TSF benchmark designed to support the evaluation of modern TSFMs. Compared with predecessors, TIME advances the field in two fundamental dimensions: **benchmark construction** and **evaluation perspective**. Benchmark construction encompasses data curation and task formulation. We first curate a diverse collection of *fresh datasets* from public sources or industry partners, which

have never/rarely been explored by existing TSF benchmarks. Secondly, to ensure data integrity, we establish a rigorous human-in-the-loop *data preparation pipeline*, which integrates automated screening with human decision to refine raw curated data into benchmark-ready quality. Critically, to ensure practical relevance, we systematically design task formulation by prioritizing alignment with the specific practical application contexts of each dataset. We leverage both domain-specific knowledge and LLM-based analysis to validate the rationality of each prediction task, ensuring that configurations (frequency and horizons) adhere to real-world operational requirements and variate predictability.

For evaluation perspective, we introduce a *pattern-level analysis* approach to facilitate generalizable and diagnostic benchmarking across heterogeneous datasets. Leveraging STL decomposition, we select a curated set of structural and interpretable time series features to characterize the intrinsic pattern of each variate. Through a binary encoding scheme, variates exhibiting identical pattern representations can be retrieved for a pattern-specific evaluation. For each TSFM, variate-level results are aggregated over retrieved variates, yielding high-level and generalizable insights into model capabilities on universal temporal behaviors.

Our contributions are summarized as follows:

- We introduce TIME, a task-centric benchmark comprising 50 fresh datasets and 98 forecasting tasks, where configurations are aligned with real-world operational requirements. By utilizing distinctively fresh data, TIME enables a strict zero-shot evaluation free from data leakage, ensuring a fair and unbiased assessment.
- We propose a pattern-level evaluation perspective for generalizable, high-level, and cross-dataset performance benchmarking. By leveraging a curated set of interpretable temporal features with clear separability, TIME enables effective pattern-based stratification and retrieval, yielding generalizable and diagnostic insights into model performance.

- We evaluate 12 representative TSFMs on TIME and develop an interactive leaderboard supporting multi-granular analysis, combining quantitative results with qualitative visualization to improve the interpretability and actionability of benchmark outcomes.

2. Related Work

2.1. Time Series Forecasting Benchmarks

We present the timeline of TSF benchmarks in Figure 2 . Early deep learning studies for TSF (Lai et al., 2018; Salinas et al., 2020) are not evaluated on standard benchmarks. Each work typically evaluates models on 4–6 datasets, which vary across studies and lack unified evaluation protocols.

A milestone is the M4 competition (Makridakis et al., 2020), which provides a large-scale univariate time series benchmark that enables evaluation of deep learning models such as MLPs and RNNs. With the rise of time series transformers (TST), LSF (Zhou et al., 2021; Wu et al., 2021) emerges as the first standardized benchmarks for long-horizon forecasting. Owing to its moderate scale and ease of use, LSF quickly becomes the most widely used in the TSF community. Concurrently, the Monash archive (Godahewa et al., 2021) introduced a diverse collection of datasets from various domains. Both LSF and Monash integrate existing and newly collected datasets, which serve as the primary data sources for many later TSF benchmarks. Afterwards, several domain-specific benchmarks are proposed, including M5 (Makridakis et al., 2022) for sales, CloudOPS (Woo et al., 2023) for cloud operation metrics, and LibCity (Wang et al., 2023) for urban transportation.

Since 2023, TSFMs have emerged as a prominent paradigm. Their rise drives the creation of large-scale benchmarks designed for zero-shot evaluation, characterized by diverse domains and extensive data coverage to assess universal forecasting capabilities (Aksu et al., 2024; Ansari et al., 2024; Li et al., 2025; Cohen et al., 2025; Shchur et al., 2025). At the same time, the community reflects on the limitations of prevalent benchmarks (Hewamalage et al., 2023; Bergmeir, 2024) and calls for a new generation of TSF evaluation, leading to a new wave of benchmark development (Qiu et al., 2024; Shao et al., 2024; Zhang et al., 2024; Ni et al., 2025). However, these recent works still face main limitations. First, while they include a larger number of datasets, they mainly assemble previously released datasets instead of incorporating genuinely new data sources, failing to expand the boundaries of evaluation across novel and diverse temporal patterns. Second, both data integrity and task formulation are often compromised, characterized by unverified data flaws and mechanical setups detached from real-world contexts. Finally, their evaluation approaches remain conventional relying on coarse dataset-level metrics.

While aggregating by metadata (e.g., domain) offers convenient categorization, it neglects intrinsic temporal patterns, failing to yield generalizable conclusions regarding model capabilities on universal dynamics.

2.2. Time Series Features

Unlike natural language or visual data, time series are inherently heterogeneous and lack intuitive semantics, making them difficult to interpret and categorize during analysis. Time series features (*tsfeatures*) are widely used to characterize the statistical and structural properties of time series. Early studies apply them primarily for classification tasks (Fulcher & Jones, 2014; Fulcher, 2018; Lubba et al., 2019) or synthetic data generation (Bahrpeyma et al., 2021). In the context of forecasting, a common practice (Kang et al., 2017; Spiliotis et al., 2020; Godahewa et al., 2021) selects several features and uses principal component analysis (PCA) to visualize the distribution of variates within a dataset. Recent benchmarks (Aksu et al., 2024; Qiu et al., 2024; Cohen et al., 2025) further employ *tsfeatures* to define several high-level properties (e.g., trend, seasonality) and analyze the overall coverage of their datasets. However, existing *tsfeature*-based analyses still remain at the dataset level, offering limited insights into pattern-specific model performance for variates across datasets.

3. Preliminary

Time Series Forecasting Benchmarks. A TSF benchmark serves as a unified platform for systematically evaluating forecasting methods. We formalize its internal structure as a hierarchy consisting of several levels: (1) A *benchmark* comprises multiple tasks that share a common evaluation protocol and provides multiple perspectives of analysis. (2) A *task* is defined by a specific dataset together with a dedicated prediction horizon. (3) A *dataset* contains one or more series, and the same underlying data sampled at different frequencies are treated as distinct datasets. (4) A *series* can be *univariate* or *multivariate*; series within the same dataset may vary in temporal length but share the same set of variates. (5) A *variante* represents a single time-dependent variable, corresponding to one univariate time series (UTS) or a channel/variable within a multivariate series (MTS). In this benchmark, all variates are treated as prediction targets, excluding exogenous covariates. (6) A *testing window* denotes a continuous segment of a time series used as ground truth target for forecasting, typically with the length of prediction horizon.

Forecasting Task. We formulate a forecasting task as $\mathcal{T} = (\mathcal{D}, H)$. Here, H denotes the prediction horizon, and $\mathcal{D} = \{\mathbf{X}^{(i)}\}_{i=1}^N$ denotes a dataset comprising N time series. Each series $\mathbf{X} \in \mathbb{R}^{L \times D}$ represents a complete temporal

record of the sequence. Formally, the series is composed of D individual variates, formulated as $\mathbf{X} = [\mathbf{x}_1, \mathbf{x}_2, \dots, \mathbf{x}_D]$. Depending on the dimension, the series is categorized as univariate if $D = 1$ or multivariate if $D > 1$. For evaluation, we isolate the last L_{test} time steps of each series as the test set. Forecasting samples are generated via a non-overlapping rolling window strategy: We employ a rolling window with a stride of H over this test period, generating $W = \lfloor L_{test}/H \rfloor$ samples per series. For the k -th sample ($1 \leq k \leq W$), the benchmark defines the testing window as $\mathbf{X}_{t_k:t_k+H} \in \mathbb{R}^{H \times D}$, where the start index is $t_k = (k-1)H$ relative to the test set.

Time Series Pattern. A time series pattern denotes the intrinsic temporal characteristics of a single variate. By abstracting raw data into patterns, it serves as a bridge for cross-dataset evaluation and enables more general, pattern-level analysis. For a given variate \mathbf{x} , we define its pattern representation as a vector $\mathbf{F} = (F_1, \dots, F_K)$ composed of a specific set of time series features. This vector encodes a specific set of statistical properties utilized to quantify the structural nature of the series, with the detailed feature selection provided in Section 5.

4. Benchmark Construction

4.1. Data Curation

Data Sources. Legacy datasets, many of which have been released for years, are likely to have been partially ingested into large-scale pre-training corpora. This exposure causes risks of both inadvertent and malicious contamination, undermining the reliability of benchmark-based evaluations. To mitigate the risk, we prioritize data novelty by curating fresh datasets. Our data are curated from four different sources. We first curate public statistics from official government portals. We also acquire real-world data through collaborations with industrial and academic partners. To expand the diversity, we also collect supplementary sequences from open-access websites and forecasting competitions. Further details are provided in Section B.

Manual Curation. For each candidate dataset, we proceed with the following procedures: Firstly, we conduct an eligibility check covering both format and context. We verify that the data are *continuous* time series with valid timestamps and a regular sampling frequency, while simultaneously ensuring that its underlying application context supports meaningful forecastable processes. Subsequently, we perform metadata-based filtering by examining the frequency and time span of each series to ensure sufficient sequence length, discarding those that are too short relative to their frequency. We also review the semantic meaning of each variable, removing those deemed irrelevant to the

application context. After that, we employ visualization-based inspection to identify and exclude variates lacking clear temporal patterns (e.g., constant sequences) or containing excessive missing values. In cases where quality is poor across the full span, we determine if a reliable shorter sub-time span can be extracted. Finally, the curated variates are organized into datasets following the structure defined in Section 3. Where appropriate, related variates are aggregated into multivariate series after aligning them to a common time span. Otherwise, they remain as multiple univariate series.

4.2. Automatic Screening

Given a raw dataset, we deploy an automated screening pipeline for fine-grained quality profiling. Instead of discarding series or variates immediately, this process generates a *Quality Summary* documenting the status of every series, proceeding through five sequential steps: (1) *Timestamp Rectification*: Curated data often exhibit missing or misaligned timestamps, which undermines temporal consistency. We first identify and fill missing timestamps, then rectify misaligned timestamps by calibrating them to the nearest standard timestamp based on the data frequency. (2) *Rule-based Validation*: As manual inspection is insufficient for fine-grained quality control at scale, we implement an automatic process to validate data against a set of predefined rules. We flag variates violating missing rate or length thresholds, and employ value dominance to identify uninformative series that exhibit negligible temporal dynamics. (3) *Statistical Test*: To eliminate unpredictable variates, we employ the Ljung-Box test (Ljung & Box, 1978) to detect white noise, which are flagged for removal. (4) *Extreme Outliers Removal*: We apply a local interquartile range (IQR) filter to detect and eliminate extreme erroneous values. For a time point t within a local window w , a value is identified as an error if it falls outside $[m_w - k \cdot \text{IQR}_w, m_w + k \cdot \text{IQR}_w]$, where m_w is the median and $\text{IQR}_w = Q_{0.75} - Q_{0.25}$. Detected errors are replaced by the preceding valid observation. We set $k = 9$ to preserve genuine spikes while filtering technical errors. (5) *Correlation Check*: Finally, we compute pairwise correlations across all variates within the dataset to detect potential redundancy. Pairs exhibiting a correlation coefficient exceeding a predefined threshold are flagged as highly collinear, marked for subsequent expert review.

After all these procedures (See C.1 for detailed algorithms), all diagnostic results are aggregated into a dataset-level Quality Summary, which is submitted for final human decision-making.

4.3. Human Decision Making

Dataset Finalization via Review. Leveraging the Quality Summary, this stage introduces human judgment to finalize

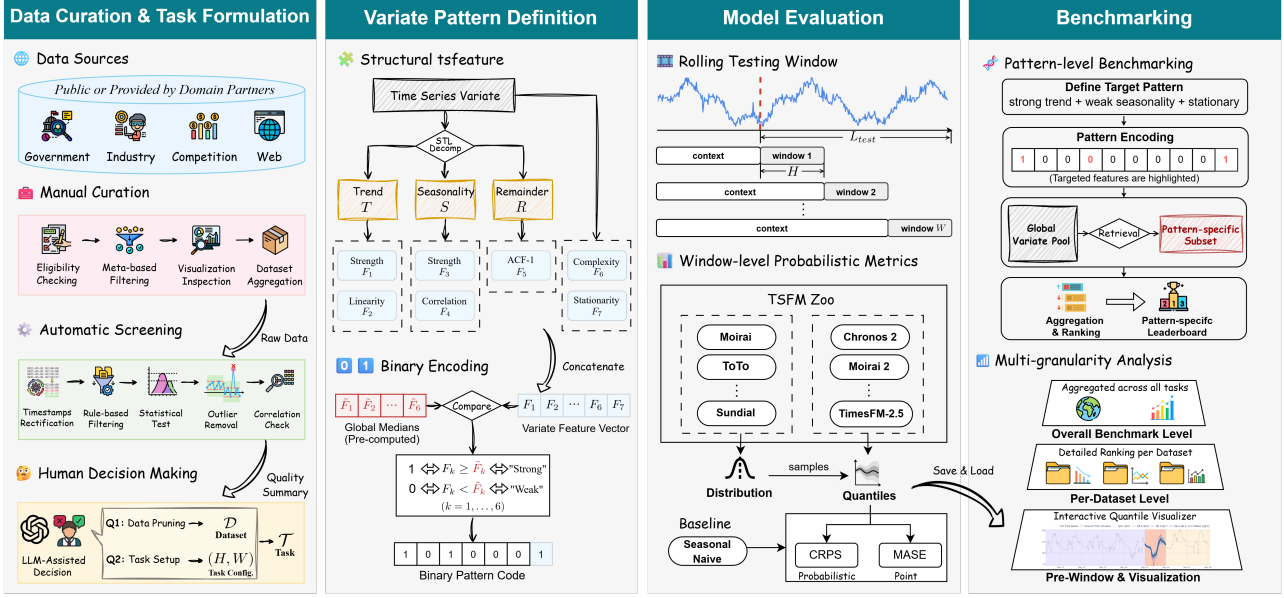


Figure 3. The overall workflow of TIME. (1) Fresh datasets are curated from diverse sources, integrating automated quality screening with LLM-assisted human decision-making to formulate context-aware forecasting tasks. (2) The intrinsic pattern of each variate is characterized by structural time series features derived via STL decomposition and mapped to binary encodings. (3) Representative TSFMs undergo rolling-window evaluations for probabilistic forecasting, where quantile-based metrics are computed and recorded for each window. (4) Performance analysis is conducted through pattern-targeted retrieval and multi-granular leaderboards.

dataset structure, resolving quality ambiguities that automated protocols cannot address alone. Guided by domain knowledge and LLM-synthesized insights, we rigorously evaluate flagged variates within their specific application contexts to distinguish between genuine data corruption and meaningful domain characteristics. For instance, while high correlation among the availabilities of different car parks suggests redundancy warranting removal, similar correlations between macroeconomic indicators reflect inherent structural dependencies that must be preserved. This review dictates the precise granularity of data pruning: we determine whether to exclude specific problematic series (series-level) or eliminate entire variates (variate-level) that are fundamentally unsuitable for forecasting. This decision process ensures each dataset \mathcal{D} maintain high data integrity while remaining aligned with real-world application.

Context-Aligned Task Formulation. A meaningful forecasting task should mirror its real-world operational requirements rather than adhere to arbitrary defaults. We posit that data frequency and task settings are intrinsically subservient to the application context. Instead of rigid settings (e.g., one-size-fit-all horizons (Wu et al., 2021), frequency-proportional horizons (Aksu et al., 2024) or fixed split ratios (Qiu et al., 2024)), we formulate each task \mathcal{T} via context-aware configurations derived from domain expertise and LLM analysis. Specifically, prediction horizons H are rigorously tailored to the dataset's frequency and application context. We define three horizons (*Short*, *Medium*, *Long*)

for applicable high-frequency scenarios, and restrict low-frequency or constrained datasets to a single, operationally viable horizon. Similarly, we calibrate the test length L_{test} to align with practical cycles (e.g., covering full seasonal periods), ensuring the evaluation framework prioritizes practical applicability.

5. Benchmarking Strategy

5.1. Structural tsfeatures for Pattern Definition

We curate a set of *structural* time series features to facilitate effective and interpretable categorization. For each variate $\mathbf{x} \in \mathbb{R}^L$, we decompose it into three additive components via STL decomposition (Seasonal and Trend decomposition using Loess) (Cleveland et al., 1990):

$$\mathbf{x} = T + S + R. \quad (1)$$

In contrast to previous benchmarks that compute metrics directly on raw variates \mathbf{x} (Aksu et al., 2024; Qiu et al., 2024), our approach isolates distinct temporal components (Trend T , Seasonality S , and Remainder R). This results in features that are not only more interpretable and structured but also exhibit reduced overlap. We provide detailed definition of each tsfeature in Section D.2

For Trend T , we select two features to reflect its significance and structural patterns. *Trend Strength* (F_1) quantifies the proportion of the variate's variability that is explained by the trend component. *Trend Linearity* (F_2) capture the structural

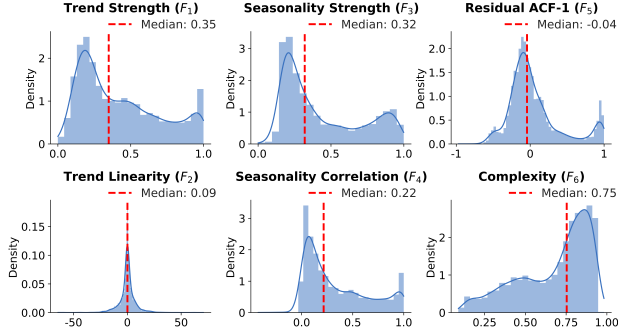


Figure 4. Empirical density distributions of our structural tsfeatures (F_1 – F_6) across the benchmark variates. *Stationarity* (F_7) is omitted here as it is a binary indicator, with non-stationary variates accounting for 7.6% of the total.

evolution of the trend, offering an intuitive metric to quantify the degree of its linear progression.

For Seasonality S , we similarly characterize its significance and structural patterns via two features. We compute *Seasonality Strength* (F_3) analogously to F_1 to quantify the seasonal contribution to the overall variability. *Seasonality Correlation* (F_4) measures the linear correlation between consecutive seasonal cycles, reflecting the stability and consistency of the seasonal evolution over time.

For Remainder R , we investigate whether any significant temporal structure persists. *Residual ACF-1* (F_5) capture residual dependencies by calculating the first-order autocorrelation of the remainder term.

Finally, we calculate two additional features on the raw variate \mathbf{x} to characterize important global patterns. We include *Complexity* (F_6 , spectral entropy of \mathbf{x}) to quantify the overall forecast difficulty, and *Stationarity* (F_7), a binary indicator derived from the Augmented Dickey-Fuller test (Dickey & Fuller, 1979) to distinguish between stationary ($p < 0.05$) and non-stationary processes.

To validate this feature set, we analyze the empirical probability distributions of these metrics across all variates in our benchmark. As shown in Figure 4, these features exhibit diverse and informative distributions (See Section D.3 for quantitative analysis), enabling effective grouping and cross-domain analysis of time series patterns regardless of the underlying dataset or sampling frequency.

5.2. Pattern-Driven Benchmarking

Based on the structural features, we propose a pattern-driven strategy to stratify the benchmark and identify variates with shared characteristics for targeted evaluation. We employ a binary encoding scheme to transform the feature vector $\mathbf{F} = [F_1, \dots, F_7]$ into a compact binary pattern code $\mathbf{B} \in \{0, 1\}^7$. Specifically, we first compute the feature vector \mathbf{F} for every variate in the benchmark. For each

Model	Date	Arch.	Param.	Multi.	Output
TimesFM 2.5	10-25	Dec.	200M	✗	Q
Chronos2	10-25	Enc.	120M	✓	Q
Kairos	09-25	E-D	23M	✗	Q
Moirai 2.0	08-25	Dec.	11M	✗	Q
VisionTS++	08-25	MAE	460M	✓	Q
TiRex	05-25	xLSTM	35M	✗	Q
Toto	05-25	Dec.	151M	✓	D
Sundial	05-25	Dec.	128M	✗	D
TimesFM 2.0	12-24	Dec.	500M	✗	Q
Chronos-bolt	11-24	E-D	205M	✗	D
Moirai	06-24	Enc.	91M	✓	D
TimesFM 1.0	05-24	Dec.	200M	✗	Q

Table 1. Properties of selected TSFMs. Dates are in MM-YY formats. Enc./Dec.=Encoder/Decoder-only, E-D=Encoder-Decoder; Multi.=Multivariate support; D=Distribution; Q=Quantiles.

continuous feature F_k ($k = 1, \dots, 6$), we calculate the population median \tilde{F}_k across all the variates to serve as a global threshold. If the feature value of a variate exceeds this threshold ($F_k > \tilde{F}_k$), we consider the variate to possess a strong or dominant presence of that characteristic (encoded as 1). Otherwise, the characteristic is deemed weak or non-significant (encoded as 0). The binary feature *Stationarity* (F_7) is directly adopted without thresholding.

For each target pattern for evaluation, we can retrieve subsets of variates that exhibit identical binary codes from the whole benchmark. By using scale-invariant metrics (MASE and CRPS), we can aggregate the variate-level results for each TSFM to derive pattern-specific performance estimates. This granular evaluation allows us to generate distinct leaderboards for each pattern, revealing model capabilities across specific temporal dynamics.

6. Experiments

6.1. Global Setup

Models and Datasets. We evaluate 12 TSFMs with diverse architectural designs across 50 datasets and 98 tasks (details in Table 2). The datasets span eight domains and feature a broad spectrum of frequencies. The evaluated models include: TimesFM (2.5/2.0/1.0) (Das et al., 2024), Moirai (2/1) (Liu et al., 2025a; Woo et al., 2024), Chronos (2/Bolt) (Ansari et al., 2025; 2024), ToTo (Cohen et al., 2025), Sundial (Liu et al., 2025b), VisionTS++ (Shen et al., 2025), Kairos (Feng et al., 2025), and TiRex (Auer et al., 2025). Model properties are summarized in Table 1.

Evaluation Protocol. As described in Section 3, we adopt a rolling evaluation protocol (Aksu et al., 2024; Shchur et al., 2025). For metrics, we employ MASE and CRPS for point and probabilistic evaluation, respectively. To accommodate two distinct output formats of TSFMs (*distribution-based* and *quantile-based*), we derive quantiles via sampling for

distribution-based models prior to metric computation, using a default sample size of 100. During evaluation, we save window-level metrics and quantile predictions per model, enabling the hierarchical analysis and visualization of the interactive leaderboard.

Metric Normalization and Aggregation. While MASE and CRPS are inherently scale-independent, evaluating TSFMs across diverse datasets presents challenges due to varying intrinsic forecastability. To ensure a robust and interpretable comparison, we adopt the protocol in (Aksu et al., 2024) and utilize a consistent relative evaluation framework where model metrics are normalized against a Seasonal Naive (S-Naive) baseline. This framework is applied across all experimental views, varying only in the granularity of the normalization unit.

For any given evaluation unit u (e.g., a task or a variate), we compute the **normalized metric** as the ratio of the model's performance to the baseline:

$$\text{Metric}_{\text{model}}^{\text{norm}}(u) = \frac{\text{Metric}_{\text{model}}(u)}{\text{Metric}_{\text{S-Naive}}(u)}, \quad (2)$$

where $\text{Metric}_{\text{model}}$ and $\text{Metric}_{\text{S-Naive}}$ are the raw metric values computed via arithmetic mean within unit u . A normalized score less than 1 indicates performance superior to S-Naive, while a value greater than 1 implies inferiority. We employ the **geometric mean** to aggregate these normalized metrics across units. This choice is critical for two reasons: (1) it offers greater robustness against outliers compared to the arithmetic mean, (2) it treats multiplicative relationships symmetrically (e.g., a model that is $2\times$ better on one task and $0.5\times$ on another yields a neutral mean of 1.0) and (3) it preserves the interpretability of the normalized scale.

6.2. Overall Performance

In this section, we assess the general capability of TSFMs by aggregating results at the **task level**, i.e., a unique pair of (dataset, horizon). The normalization unit here is the task itself: we first compute the raw metrics for a task (averaged across rolling windows, variates and series), normalize them by the corresponding S-Naive task score, and then aggregate these normalized scores across all 98 tasks using the geometric mean. Detailed numerical and Per Dataset results can be found in Table 4 and Table 6, respectively.

Results. Figure 5 illustrates the overall performance on point and probabilistic forecasting across all tasks. TimesFM-2.5 achieves the lowest MASE, while Chronos2 leads in probabilistic forecasting with the best CRPS. A distinct performance progression is observed where newer iterations (e.g., TimesFM-2.5 vs. 2.0/1.0, and Moirai2 vs. Moirai, Chronos2 vs. Chronos-bolt) consistently outperform their predecessors. This confirms that recent advance-

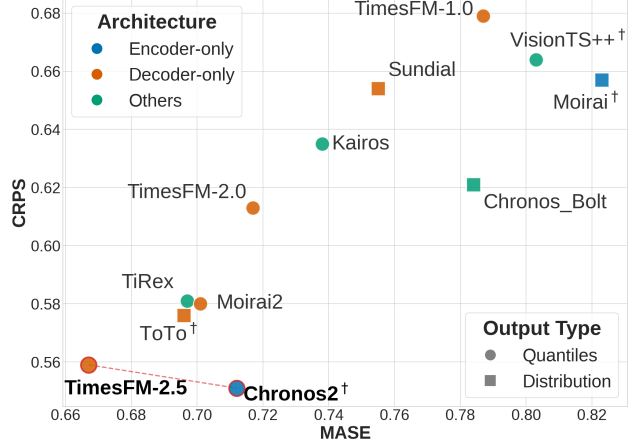


Figure 5. Overall performance across all tasks. Task-level results are normalized by the *Seasonal Naive* baseline and aggregated using the geometric mean. Lower values (bottom-left corner) indicate better performance. Models annotated with \dagger support multivariate modeling, whereas others operate under channel independence.

ments in TSFMs represent genuine capability improvements rather than overfitting to the data bias in established benchmarks. Analyzing the profile of the top-5 performing models reveals distinct design trends: decoder-only frameworks (TimesFM-2.5, ToTo, Moirai2) and quantile-based mechanisms are widely adopted. Notably, the leading positions are generally occupied by the most recently released models. This trend not only highlights the development of the TSFM field but also validates the rationality of our benchmark in accurately capturing these genuine advancements.

6.3. Pattern-specific Performance

Unlike the overall evaluation, pattern-driven analysis requires granular insights at the **variety level**. For a target pattern (e.g., high trend strength), we utilize our retrieval system to identify all variates matching this criterion from the benchmark. The performance for a specific pattern is then computed as the geometric mean of the scaled metrics across all retrieved variates. In this section, we analyze six essential tsfeature independently. Figure 6 presents the Normalized MASE gap between time series exhibiting a specific feature ($F_k = 1$, red dots) and those that do not ($F_k = 0$, blue dots), while CRPS can be found in Figure 8. While joint patterns are possible, we focus on single-feature impacts to provide clear, actionable insights, encouraging readers to explore complex combinations via our leaderboard. Full numerical results are provided in Table 5.

Trend. The impact of trend attributes reveals a consistent performance profile. Regarding Trend Strength (F_1), for most models, we observe that the relative improvement over the S-Naive baseline is more pronounced on variates with stronger trends than those with weaker ones. (indicated by

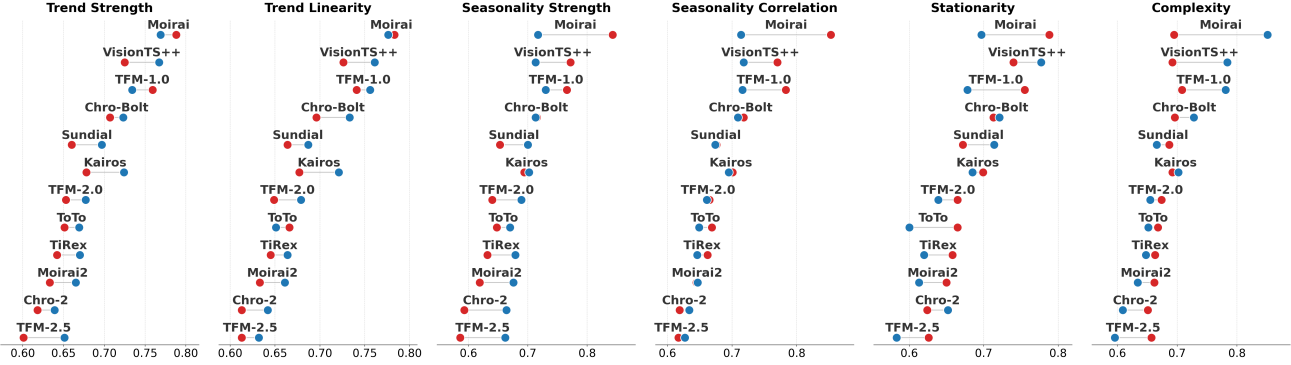


Figure 6. Comparison of MASE across different feature-specific variates. Each row represents a model’s performance on variates with $F_k = 1$ (red) and $F_k = 0$ (blue). The distance between dots indicates the performance difference of the model to that specific feature.

the red markers consistently outperforming the blue markers). The results for Trend Linearity (F_2) follow a similar pattern, where most models exhibit larger relative gains on sequences with high linearity. While TSFMs capitalize more effectively on strong and linear trending signals, the consistent performance enhancements observed across all trend-specific variates as models evolve suggest that the overall progress of TSFMs remains relatively independent of trend intensity or structure.

Seasonality. Regarding Seasonality Strength (F_3), we observe a disparity in model performance differentiation: On variates with weak seasonality, the performance gap between models is relatively narrow, where most TSFMs cluster around an MASE of 0.7. While TSFMs consistently provide a robust performance advantage over S-Naive, achieving significant further differentiation between models on such data remains challenging. In contrast, a significant divergence appears on variates exhibiting strong seasonality. The increased spread in performance on highly seasonal data suggests that a key advantage of superior models lies in their enhanced capacity to capture and model strong seasonal signals, whereas weaker models struggle to leverage this information effectively.

In terms of Seasonality Correlation (F_4), the evolution of TSFMs brings performance gains across both stable and unstable seasonal patterns. For early/weaker models (Moirai, VisionTS++, and TimesFM-1.0), the modeling effectiveness on stable periods is relatively close to that of S-Naive, which results in a significant gap compared to the much larger gains seen on unstable sequences. With further development, this gap has narrowed significantly. Most recent TSFMs show a relatively small performance difference between stable and unstable sequences. For leading models like TimesFM-2.5 and Chronos2, the performance gains on stable sequences actually surpass those on unstable ones. This suggests that recent TSFMs have become more robust to seasonality stability and provide consistent improvements.

Stationarity. For the majority of TSFMs, the relative gains are more pronounced on non-stationary sequences. This trend highlights the limitations of S-Naive, which struggle to adapt to the shifting statistical properties of non-stationary data. TSFMs, however, demonstrate a robust capacity to model these dynamic changes, resulting in a larger performance gap over the baseline in non-stationary scenarios. Notably, the model rankings exhibit high sensitivity to stationarity. For instance, ToTo ranks second on non-stationary data but drops to fifth on stationary sequences. Conversely, Chronos2 dominates stationary sequences as the top performer but falls to sixth place when dealing with non-stationary data. This shift suggests that different TSFMs possess unique inductive biases, with some optimized for handling non-stationary shifts and others prioritizing precision in stationary dynamics.

Complexity. Similar to F_3 , we observe that the inter-model disparity is noticeably smaller on variates with high complexity compared to those with low complexity. This suggests that high spectral entropy acts as a performance equalizer, compressing the variance between models, whereas lower complexity allow superior models to more clearly distinguish themselves from weaker counterparts. For weaker models, the relative gains on low-complexity data are smaller than on high-complexity sequences, indicating that their performance on simple signals shows no significant advantage over S-Naive. As models evolve, the relative improvement on low-complexity sequences increases significantly and eventually surpasses the gains seen on complex data. While high-complexity sequences remain difficult for all models, the most advanced TSFMs distinguish themselves by their superior ability to model and refine structured non-complex patterns.

Summary. Although model rankings exhibit specific variations across different pattern variates, the overall profile remains largely consistent. In most cases, TimesFM-2.5 and Chronos-2 maintain their status as the top two performers,

while Moirai2, TiRex and ToTo typically fluctuate within the third to fifth positions. Notably, we find that these feature-specific rankings do not align with the overall rankings presented in Section 6.2. While task-level aggregation is the common practice in existing benchmarks (Aksu et al., 2024; Shchur et al., 2025), our first attempt at variate-level aggregation reveals that rankings are significantly influenced by the level of aggregation. Determining the most appropriate aggregation level remains an open question, highlighting that a single leaderboard ranking is not the sole metric for success and requires more granular quantitative analysis.

6.4. Qualitatively Analysis

Beyond quantitative metrics, our platform enables qualitative analysis via prediction visualization. As shown in Section F, we observe that variates may exhibit distinct patterns in global and local views. For instance, apparent global spikes can resolve into periodicities at a local scale. Additionally, variates often combine multiple structural patterns. Regarding model behavior, TSFMs generally predict clear seasonality and trends well. However, for series with high variations, TSFMs are prone to producing conservative predictions (i.e., relatively constant lines). In such cases, these flat forecasts may statistically yield competitive MASE or CRPS scores. However, quantitative metrics alone cannot distinguish whether the model has successfully captured the underlying dynamics or merely defaulted to a safe, conservative mean. This ambiguity highlights the necessity of visual verification to interpret the true nature of model behavior.

7. Conclusion

We introduce TIME, a task-centric benchmark designed to address the limitations in data freshness, integrity, and evaluation granularity plaguing current TSFM assessments. By implementing a rigorous data pipeline, we construct a contamination-free repository of 50 fresh datasets with context-aligned task formulations. Our pattern-level evaluation perspective offers granular, generalizable insights into intrinsic model capabilities, revealing that TSFMs exhibit significant advantages over Seasonal Naive baseline in handling variates with non-stable seasonality or non-stationarity. Crucially, visualization serves as an essential complement, validating whether statistical predictive quality truly translates into actionable reliability for real-world applications. In future iterations, we plan to incorporate task-specific metrics tailored to different applications.

References

Aksu, T., Woo, G., Liu, J., Liu, X., Liu, C., Savarese, S., Xiong, C., and Sahoo, D. Gift-eval: A benchmark for general time series forecasting model evaluation. *arXiv preprint arXiv:2410.10393*, 2024.

preprint arXiv:2410.10393, 2024.

Ansari, A. F., Stella, L., Turkmen, C., Zhang, X., Mercado, P., Shen, H., Shchur, O., Rangapuram, S. S., Pineda Arango, S., Kapoor, S., Zschiegner, J., Mad-dix, D. C., Mahoney, M. W., Torkkola, K., Gordon Wilson, A., Bohlke-Schneider, M., and Wang, Y. Chronos: Learning the language of time series. *Transactions on Machine Learning Research*, 2024. ISSN 2835-8856. URL <https://openreview.net/forum?id=gerNCVqqTR>.

Ansari, A. F., Shchur, O., Küken, J., Auer, A., Han, B., Mercado, P., Rangapuram, S. S., Shen, H., Stella, L., Zhang, X., et al. Chronos-2: From univariate to universal forecasting. *arXiv preprint arXiv:2510.15821*, 2025.

Auer, A., Podest, P., Klotz, D., Böck, S., Klambauer, G., and Hochreiter, S. Tirex: Zero-shot forecasting across long and short horizons with enhanced in-context learning. In *The Thirty-ninth Annual Conference on Neural Information Processing Systems*, 2025. URL <https://openreview.net/forum?id=v7UqniC9pF>.

Bahrpeyma, F., Roantree, M., Cappellari, P., Scriney, M., and McCarren, A. A methodology for validating diversity in synthetic time series generation. *MethodsX*, 8:101459, 2021.

Bergmeir, C. Fundamental limitations of foundational forecasting models: The need for multimodality and rigorous evaluation. In *Proc. NeurIPS Workshop*, 2024.

Brigato, L., Morand, R., Strømmen, K. J., Panagiotou, M., Schmidt, M., and Mougiaakou, S. There are no champions in supervised long-term time series forecasting. *Transactions on Machine Learning Research*, 2026. ISSN 2835-8856. URL <https://openreview.net/forum?id=y01JuBpTBB>.

Carlini, N., Ippolito, D., Jagielski, M., Lee, K., Tramer, F., and Zhang, C. Quantifying memorization across neural language models. In *The Eleventh International Conference on Learning Representations*, 2022.

Cleveland, R. B., Cleveland, W. S., McRae, J. E., Terpenning, I., et al. Stl: A seasonal-trend decomposition. *J. off. Stat*, 6(1):3–73, 1990.

Cohen, B., Khwaja, E., Doubli, Y., Lemaachi, S., Lettieri, C., Masson, C., Miccinilli, H., Ramé, E., Ren, Q., Rostamizadeh, A., et al. This time is different: An observability perspective on time series foundation models. *arXiv preprint arXiv:2505.14766*, 2025.

Cohen, J. *Statistical power analysis for the behavioral sciences*. routledge, 2013.

Das, A., Kong, W., Sen, R., and Zhou, Y. A decoder-only foundation model for time-series forecasting. In *Forty-first International Conference on Machine Learning*, 2024.

Dickey, D. A. and Fuller, W. A. Distribution of the estimators for autoregressive time series with a unit root. *Journal of the American statistical association*, 74(366a): 427–431, 1979.

Feng, K., Lan, S., Fang, Y., He, W., Ma, L., Lu, X., and Ren, K. Kairos: Towards adaptive and generalizable time series foundation models. *arXiv preprint arXiv:2509.25826*, 2025.

Fulcher, B. D. Feature-based time-series analysis. In *Feature engineering for machine learning and data analytics*, pp. 87–116. CRC press, 2018.

Fulcher, B. D. and Jones, N. S. Highly comparative feature-based time-series classification. *IEEE Transactions on Knowledge and Data Engineering*, 26(12):3026–3037, 2014.

Garza, F., Canseco, M. M., Challú, C., and Olivares, K. G. Statsforecast: Lightning fast forecasting with statistical and econometric models. *PyCon Salt Lake City, Utah, US*, 2022:66, 2022.

Godahewa, R., Bergmeir, C., Webb, G. I., Hyndman, R. J., and Montero-Manso, P. Monash time series forecasting archive. In *Neural Information Processing Systems Track on Datasets and Benchmarks*, 2021.

Hewamalage, H., Ackermann, K., and Bergmeir, C. Forecast evaluation for data scientists: common pitfalls and best practices. *Data Mining and Knowledge Discovery*, 37(2): 788–832, 2023.

Jurado, K., Ludvigson, S. C., and Ng, S. Measuring uncertainty. *American Economic Review*, 105(3):1177–1216, 2015.

Kang, Y., Hyndman, R. J., and Smith-Miles, K. Visualising forecasting algorithm performance using time series instance spaces. *International Journal of Forecasting*, 33 (2):345–358, 2017.

Lago, J., Marcjasz, G., De Schutter, B., and Weron, R. Forecasting day-ahead electricity prices: A review of state-of-the-art algorithms, best practices and an open-access benchmark. *Applied Energy*, 293:116983, 2021.

Lai, G., Chang, W.-C., Yang, Y., and Liu, H. Modeling long-and short-term temporal patterns with deep neural networks. In *The 41st international ACM SIGIR conference on research & development in information retrieval*, pp. 95–104, 2018.

Li, Z., Qiu, X., Chen, P., Wang, Y., Cheng, H., Shu, Y., Hu, J., Guo, C., Zhou, A., Jensen, C. S., et al. Tsfm-bench: A comprehensive and unified benchmark of foundation models for time series forecasting. In *Proceedings of the 31st ACM SIGKDD Conference on Knowledge Discovery and Data Mining V. 2*, pp. 5595–5606, 2025.

Liu, C., Aksu, T., Liu, J., Liu, X., Yan, H., Pham, Q., Sahoo, D., Xiong, C., Savarese, S., and Li, J. Moirai 2.0: When less is more for time series forecasting. *arXiv preprint arXiv:2511.11698*, 2025a.

Liu, G., Liu, J., Bai, Y., Wang, C., Wang, H., Zhao, H., Liang, G., Zhao, J., and Qiu, J. Eweld: A large-scale industrial and commercial load dataset in extreme weather events. *Scientific data*, 10(1):615, 2023.

Liu, Y., Qin, G., Shi, Z., Chen, Z., Yang, C., Huang, X., Wang, J., and Long, M. Sundial: A family of highly capable time series foundation models. *arXiv preprint arXiv:2502.00816*, 2025b.

Ljung, G. M. and Box, G. E. On a measure of lack of fit in time series models. *Biometrika*, 65(2):297–303, 1978.

Lubba, C. H., Sethi, S. S., Knaute, P., Schultz, S. R., Fulcher, B. D., and Jones, N. S. catch22: Canonical time-series characteristics: Selected through highly comparative time-series analysis. *Data mining and knowledge discovery*, 33(6):1821–1852, 2019.

Ludvigson, S. C., Ma, S., and Ng, S. Uncertainty and business cycles: exogenous impulse or endogenous response? *American Economic Journal: Macroeconomics*, 13(4): 369–410, 2021.

Makridakis, S., Spiliotis, E., and Assimakopoulos, V. The m4 competition: 100,000 time series and 61 forecasting methods. *International Journal of Forecasting*, 36(1): 54–74, 2020.

Makridakis, S., Spiliotis, E., and Assimakopoulos, V. The m5 competition: Background, organization, and implementation. *International Journal of Forecasting*, 38(4): 1325–1336, 2022.

Ni, J., Wang, S., Liu, Z., Shi, X., Zhong, X., Ye, Z., and Jin, W. U-cast: Learning hierarchical structures for high-dimensional time series forecasting. *arXiv preprint arXiv:2507.15119*, 2025.

Qiu, X., Hu, J., Zhou, L., Wu, X., Du, J., Zhang, B., Guo, C., Zhou, A., Jensen, C. S., Sheng, Z., and Yang, B. Tfb: Towards comprehensive and fair benchmarking of time series forecasting methods. *Proc. VLDB Endow.*, 17(9): 2363–2377, 2024.

Salinas, D., Flunkert, V., Gasthaus, J., and Januschowski, T. Deepar: Probabilistic forecasting with autoregressive recurrent networks. *International journal of forecasting*, 36(3):1181–1191, 2020.

Shao, Z., Wang, F., Xu, Y., Wei, W., Yu, C., Zhang, Z., Yao, D., Sun, T., Jin, G., Cao, X., et al. Exploring progress in multivariate time series forecasting: Comprehensive benchmarking and heterogeneity analysis. *IEEE Transactions on Knowledge and Data Engineering*, 2024.

Shchur, O., Ansari, A. F., Turkmen, C., Stella, L., Erickson, N., Guerron, P., Bohlke-Schneider, M., and Wang, Y. fev-bench: A realistic benchmark for time series forecasting. *arXiv preprint arXiv:2509.26468*, 2025.

Shen, L., Chen, M., Liu, X., Fu, H., Ren, X., Sun, J., Li, Z., and Liu, C. Visions++: Cross-modal time series foundation model with continual pre-trained vision backbones. *arXiv preprint arXiv:2508.04379*, 2025.

Spiliotis, E., Kouloumos, A., Assimakopoulos, V., and Makridakis, S. Are forecasting competitions data representative of the reality? *International Journal of Forecasting*, 36(1):37–53, 2020.

Wang, J., Jiang, J., Jiang, W., Han, C., and Zhao, W. X. Towards efficient and comprehensive urban spatial-temporal prediction: A unified library and performance benchmark. *arXiv e-prints*, pp. arXiv–2304, 2023.

Woo, G., Liu, C., Kumar, A., and Sahoo, D. Pushing the limits of pre-training for time series forecasting in the cloudops domain. *arXiv preprint arXiv:2310.05063*, 2023.

Woo, G., Liu, C., Kumar, A., Xiong, C., Savarese, S., and Sahoo, D. Unified training of universal time series forecasting transformers. In *Forty-first International Conference on Machine Learning*, 2024.

Wu, H., Xu, J., Wang, J., and Long, M. Autoformer: Decomposition transformers with Auto-Correlation for long-term series forecasting. In *Advances in Neural Information Processing Systems*, 2021.

Zhang, J., Wen, X., Zhang, Z., Zheng, S., Li, J., and Bian, J. Probs: Benchmarking point and distributional forecasting across diverse prediction horizons. *Advances in Neural Information Processing Systems*, 37:48045–48082, 2024.

Zhang, Z., Lin, L., Gao, S., et al. A machine learning model for hub-height short-term wind speed prediction. *Nature Communications*, 16:3195, 2025. doi: 10.1038/s41467-025-58456-4. URL <https://doi.org/10.1038/s41467-025-58456-4>.

Zhou, H., Zhang, S., Peng, J., Zhang, S., Li, J., Xiong, H., and Zhang, W. Informer: Beyond efficient transformer for long sequence time-series forecasting. In *Proceedings of the AAAI conference on artificial intelligence*, volume 35, pp. 11106–11115, 2021.

A. Further Discussion of Our Motivation

A.1. Plateaued Performance and Benchmark Contamination

Unlike natural language tasks, time-series forecasting lacks a human evaluation standard that can serve as an upper-bound reference. As a result, the validity of benchmarks can only be assessed indirectly through relative performance trends across models. In this context, as illustrated in the Figure 1, performance gains on current popular benchmarks have continued to slow down, making it increasingly difficult to disentangle genuine modeling progress from apparent improvements driven by the noise, implementation details, or data biases of evaluation benchmark.

A key factor contributing to this ambiguity is the growing risk of benchmark contamination in TSFMs. Most existing TSFM benchmarks rely on publicly available datasets, many of which have been released for years and are likely to have been partially absorbed into large-scale pretraining corpora. Given the demonstrated ability of foundation models to memorize training data (Carlini et al., 2022), both inadvertent and malicious contamination may occur, undermining the reliability of benchmark-based evaluation.

Notably, benchmark contamination in time series settings is arguably more difficult to detect and mitigate than in natural language. Time series data lacks intuitive semantic structure, making leakage hard to identify through manual inspection or standard similarity-based filtering. In addition, fragmented dataset versioning and inconsistent naming conventions often obscure shared data origins, leading to unintentional overlap across benchmarks. Finally, strong temporal dependencies imply that even datasets drawn from disjoint time periods may still exhibit implicit information leakage. Taken together, these factors suggest that contamination can silently inflate benchmark performance, further obscuring whether observed gains reflect genuine modeling advances or merely apparent improvements.

A.2. Limited Evaluation Perspective

Benchmarks are not merely tools for ranking models, but are intended to serve as interpretable references that clarify how progress should be understood and acted upon. This role is particularly critical in time series forecasting, where commonly used error metrics, such as mean squared error, lack intuitive meaning in isolation. A numerical improvement on a benchmark offers little guidance on whether a model's predictions are reliable, robust, or suitable for real-world deployment, leaving a substantial gap between benchmark performance and practical decision-making.

This gap is further exacerbated by how existing general-purpose benchmarks are structured. Evaluation results are typically organized using predefined meta-categories, such as domain labels or dataset frequency, implicitly assuming that these categories align with forecasting task characteristics and model behavior. In practice, however, temporal patterns that govern predictability—such as trend strength, seasonality, and regime changes—often cut across domains, while datasets within the same domain can exhibit substantial heterogeneity. As a result, domain-level performance comparisons provide limited insight into why a model performs well and offer weak guidance for selecting models in concrete application scenarios.

Consequently, even when benchmark performance improves, it remains unclear whether such gains reflect meaningful advances in modeling capability or merely artifacts of evaluation design. This ambiguity is amplified by the inherent difficulty of mapping scalar error values to deployment readiness: unlike many natural language benchmarks, where metrics such as accuracy can be intuitively interpreted and sometimes anchored to human-level references, commonly used time-series error measures lack a clear operational meaning. Although recent benchmarks have proposed relative evaluation schemes, such as comparisons against naive baselines or win-rate statistics across models, these normalized metrics remain abstract and provide limited intuition about whether predictions are practically usable in real temporal settings. Without interpretability grounded in temporal behavior, benchmarks risk obscuring the relationship between measured performance and real-world usability.

To address this gap, we propose an interpretability-oriented benchmark analysis that complements aggregate metrics with pattern-aware aggregation and qualitative inspection. By extracting interpretable time-series features, such as trend and seasonality strength, and grouping test instances accordingly, our analysis enables more meaningful comparisons of model behavior across distinct temporal regimes. In addition, recognizing the inherent difficulty of mapping scalar error values to deployment readiness, we provide an interactive visualization interface that allows users to directly examine model forecasts at multiple temporal scales. While this analysis does not yield a definitive deployment criterion, it offers a transparent and intuitive lens for contextualizing benchmark results and assessing model behavior in realistic temporal settings.

Table 2. Individual statistics of tasks across all datasets. **Freq** denotes the sampling frequency: T (Minute), H (Hour), D (Day), B (Business day), W (Week), M (Month), and Q (Quarter). **H** represents the forecast horizon length, and **W** represents the number of rolling test windows. Values in parentheses indicate the actual physical time duration corresponding to the time steps (e.g., 1,440 (15D) denotes 1,440 steps spanning 15 days). Blank entries in the Medium/Long-term columns indicate that the dataset is evaluated under a single task configuration.

Dataset	Freq	# Series	# Variate	Series Length				Short-term		Med-term		Long-term		Domain	Source	
				# Obs	Avg	Min	Max	Test	H	W	H	W	H	W		
Water Quality-Darwin	15T	7	6	639,618	15,229	8,662	18,985	1,440 (15D)	16 (4H)	90	96 (D)	15	288 (3D)	5	Nature	IMOS
Current Velocity	5T	1	6	158,916	26,486	26,486	32,486	4,320 (15D)	36 (3H)	120	288 (D)	15	864 (3D)	5	Nature	IMOS
Current Velocity	10T	10	6	1,239,966	20,669	7,481	31,957	2,160 (15D)	18 (3H)	120	144 (D)	15	432 (3D)	5	Nature	IMOS
Current Velocity	15T	5	6	255,096	8,503	3,710	17,953	1,440 (15D)	12 (3H)	120	96 (D)	15	288 (3D)	5	Nature	IMOS
Current Velocity	20T	27	6	1,046,550	6,460	2,529	16,759	1,080 (15D)	9 (3H)	120	72 (D)	15	216 (3D)	5	Nature	IMOS
Current Velocity	H	21	6	441,288	3,502	2,208	5,587	672 (4W)	24 (D)	28	168 (W)	4	336 (2W)	2	Nature	IMOS
CPHL	15T	2	1	20,752	10,831	9,956	10,394	1,440 (15D)	12 (3H)	120	96 (D)	15	288 (3D)	5	Nature	IMOS
CPHL	30T	2	1	26,802	14,687	11,808	17,566	1,440 (30D)	12 (3H)	120	48 (D)	30	144 (3D)	10	Nature	IMOS
CPHL	H	4	1	19,191	4,971	2,490	8,783	672 (4W)	24 (D)	28	168 (W)	4	336 (2W)	2	Nature	IMOS
Coastal T-S	5T	18	3	3,704,598	68,604	44,614	105,408	4,320 (15D)	36 (3H)	120	288 (D)	15	864 (3D)	5	Nature	IMOS
Coastal T-S	15T	5	3	313,053	20,870	16,686	23,134	1,440 (15D)	12 (3H)	120	96 (D)	15	288 (3D)	5	Nature	IMOS
Coastal T-S	20T	1	3	24,594	8,198	8,198	8,198	1,080 (15D)	9 (3H)	120	72 (D)	15	216 (3D)	5	Nature	IMOS
Coastal T-S	H	24	3	395,193	5,489	2,733	8,784	672 (4W)	24 (D)	28	168 (W)	4	336 (2W)	2	Nature	IMOS
SG Weather	D	6	4	73,488	2,953	2,953	2,953	366 (1Y)	3 (3D)	122	7 (W)	53	14 (2W)	27	Nature	data.gov.sg
SG PM 2.5	H	1	5	186,790	38,688	38,688	38,688	2,08 (3M)	24 (D)	92	72 (D)	30	168 (W)	13	Nature	data.gov.sg
NE China Wind	H	1	4	35,056	8,764	8,764	8,764	720 (30D)	24 (D)	30	72 (D)	10	168 (W)	4	Nature	Github
Australia Solar	H	1	3	85,982	35,064	35,064	35,064	2,520 (15W)	24 (D)	105	72 (D)	35	168 (W)	15	Energy	Pvoutput
EPF Electricity Price	H	5	1	262,080	52,416	52,416	52,416	2,520 (15W)	24 (D)	105	72 (D)	35	168 (W)	15	Energy	Academic
OpenElectricity NEM	5T	1	10	434,880	43,488	43,488	43,488	4,032 (2W)	24 (2H)	168	96 (8H)	42	288 (D)	14	Energy	OpenElectricity
EWELD Load	15T	1	10	205,440	20,544	20,544	20,544	1,344 (2W)	24 (4H)	56	96 (D)	14	672 (W)	2	Energy	Academic
SG Carpark	15T	354	1	5,073,528	14,332	14,332	14,332	672 (1W)	16 (4H)	42	96 (D)	7	672 (W)	1	Transportation	data.gov.sg
Finland Traffic	15T	1	1	35,136	35,136	35,136	35,136	2,976 (M)	16 (4H)	186	96 (D)	31	672 (W)	4	Transportation	Digitraffic
Port Activity	D	99	2	421,146	2,127	2,127	2,127	365 (A)	30 (M)	12					Transportation	Competition
Port Activity	W	99	2	60,192	304	304	304	52 (A)	13 (Q)	4					Transportation	Competition
ECDC COVID	D	9	1	9,681	1,117	794	1,229	150 (120D)	30 (30D)	5					Healthcare	ECDC
ECDC COVID	W	16	1	2,609	165	114	196	52 (52W)	13 (Q)	4					Healthcare	ECDC
Global Influenza	W	15	4	12,105	205	154	210	52 (52W)	13 (Q)	4					Healthcare	WHO
Crypto	D	1	4	11,344	2,842	2,842	2,842	273 (9M)	30 (M)	9					Finance	FRED
US Term Structure	B	1	40	357,400	9,327	9,327	9,327	717 (11Q)	20 (4W)	35					Finance	FRED
Oil Price	B	1	12	57,312	5,035	5,035	5,035	717 (11Q)	20 (4W)	35					Finance	FRED
Job Claims	W	1	2	392	196	196	196	52 (A)	13 (Q)	4					Economics	FRED
Uncertainty-1M	M	1	3	2,340	780	780	780	42 (42M)	6 (6M)	7					Economics	FRED
Housing Inventory	M	1	4	456	114	114	114	36 (3A)	12 (A)	3					Economics	FRED
JOLTS	M	1	6	1,782	297	297	297	60 (5A)	12 (A)	5					Economics	FRED
US Labor	M	1	14	5,320	380	380	380	60 (5A)	12 (A)	5					Economics	FRED
Vehicle Supply	M	1	6	2,346	391	391	391	60 (5A)	12 (A)	5					Economics	FRED
Auto Production-SF	M	1	1	367	367	367	367	60 (5A)	12 (A)	5					Economics	FRED
Commodity Production	M	32	1	10,403	325	120	648	60 (5A)	12 (A)	5					Economics	FRED
Commodity Import	M	8	1	5,578	697	254	1240	60 (5A)	12 (A)	5					Economics	FRED
WUI-Global	Q	1	15	4,325	294	294	294	20 (5A)	4 (A)	5					Economics	FRED
Global Price	Q	1	60	8,464	142	142	142	20 (5A)	4 (A)	5					Economics	FRED
Vehicle Sales	M	1	10	5,960	596	596	596	60 (5A)	12	5					Sales	FRED
Online Retail II	D	1	1	739	739	739	739	180 (6M)	30	6					Sales	Competition
Supply Chain-Customer	D	1	36	72,252	2,007	2,007	2,007	365 (A)	30	12					Sales	Competition
Supply Chain-Location	D	1	51	102,357	2,007	2,007	2,007	365 (A)	30	12					Sales	Competition
Azure2019-D	5T	989	3	25,596,372	8,627	8,073	8,639	864 (3D)	288 (D)	3					CloudOPS	Github
Azure2019-I	5T	492	3	12,738,438	8,630	8,250	8,639	864 (3D)	288 (D)	3					CloudOPS	Github
Azure2019-U	5T	78	3	329,019	1,406	882	2,006	288 (D)	48 (4H)	6					CloudOPS	Github
Smart Manufacturing	H	34	5	201,325	1,666	1,661	1,667	336 (2W)	24 (D)	14	168 (W)	2	336 (2W)	1	Industry	Competition
MetroPT-3	5T	1	6	88,572	17,809	17,809	17,809	1,728 (6D)	48 (4H)	36	288 (D)	6	576 (2D)	3	Industry	Competition

B. Datasets

B.1. Nature

Water Quality-Darwin This dataset consists of water quality measurements sourced from the National Reference Station (NRSDAR) located off the coast of Darwin, Northern Territory. It features multivariate time series from seven stations, downsampled to a 15-minute resolution. The dataset tracks six key water quality indicators: electrical conductivity (CNDC), temperature (TEMP), practical salinity (PSAL), chlorophyll mass concentration (CPHL), turbidity (TURB), and dissolved oxygen (DOX2). We ensured data integrity by filtering out bad-quality data points based on the provided quality flags. Data was sourced from Australia's Integrated Marine Observing System (IMOS) - IMOS is enabled by the National Collaborative Research Infrastructure Strategy (NCRIS). The support of the Darwin Port Corporation is also acknowledged.

Current Velocity This dataset consists of time-series observations of ocean current velocities sourced from the National Mooring Network Facility, designed to monitor oceanographic phenomena in Australian coastal waters. The data were collected using Acoustic Doppler Current Profilers (ADCP) hosted on moorings across New South Wales, the Northern Territory, Queensland, South Australia, and Western Australia. The observational period covers May 22, 2020, to August 16, 2024. We select the primary flow indicators including the zonal (UCUR), meridional (VCUR), and vertical (WCUR) current

velocity components. Additionally, environmental parameters such as sea water temperature (TEMP), pressure (PRES), and sound speed (SSPD) are included to characterize the hydrographic conditions at the instrument depth. Data with different minute-level sampling frequencies originate from distinct measurement stations. The hourly-level data were obtained by downsampling these minute-level records, filtering out sequences that were too short

CPHL This dataset monitors chlorophyll mass concentration across four marine stations in Australia. The data collection falls within the overall span of January 1, 2021 to January 1, 2023, though the specific temporal coverage varies for each station within this period. Regarding sampling frequency, two stations record at 15-minute intervals, while the remaining two operate at 30-minute intervals. The hourly-level dataset was derived by downsampling the minute-level records.

Coastal T-S This dataset is derived from the National Mooring Network Facility, which maintains a series of reference stations for monitoring Australian coastal waters. We collected time-series observations of temperature and salinity from dozens of stations within this network. The dataset covers the period from January 1, 2023, to January 1, 2024, utilizing high-precision measurements from temperature loggers and Conductivity-Temperature-Depth (CTD) instruments to capture coastal oceanographic variations. Same as above, distinct minute-level frequencies originate from different stations, while hourly data are derived via downsampling

SG Weather This dataset is curated from the real-time daily weather readings collected from six monitoring stations across Singapore. We select four variates featuring temperature, humidity, wind direction, and wind speed. We curated the data recording from January 1, 2017, to January 31, 2025 via the official API. Observations from February 1, 2024, onwards are used as the test set.

SG PM 2.5 This dataset captures hourly concentrations of PM2.5 across five major geographical regions in Singapore: Central, East, North, South, and West. The observational data covers the period from January 1, 2021, to May 31, 2025, reflecting regional air quality dynamics. Data from the final year was utilized as the test set.

NE China Wind We utilize the meteorological recordings from (Zhang et al., 2025), covering Northeast China at an hourly frequency. Key variables include u-wind, v-wind, geopotential height, and temperature. While the original work (Zhang et al., 2025) utilized the latter two as auxiliary features, we treat all four variables as target series for forecasting. Due to data homogeneity, we only use data from a single region spanning one year.

B.2. Energy

Australia Solar This dataset is curated from PVOutput and Solcast¹ platforms. It comprises hourly solar energy generation records from three distinct photovoltaic (PV) stations located in Australia. The temporal coverage spans exactly four years, from April 1, 2021, to March 31, 2025.

EPF Electricity Price This dataset is sourced from (Lago et al., 2021) includes hourly electricity markets recording from five different areas, each of them comprising 6 years of data. In this benchmark, we discard all exogenous variables and exclusively retain the electricity price as the prediction target.

OpenElectricity NEM This dataset is curated from the OpenElectricity platform, a public repository tracking energy statistics across Australia. We focus specifically on the National Electricity Market (NEM), collecting electricity demand and price series from five distinct regions. The data covers the period from January 1, 2025, to May 31, 2025.

EWELD Load This dataset is sourced from (Liu et al., 2023), which includes 15-minute electricity consumption data from industrial and commercial users under extreme weather events. We select a subset of 10 users spanning from June 1, 2019, to December 31, 2019. We utilize only the univariate consumption series and exclude all weather covariates.

B.3. Transportation

SG Carpark This dataset tracks parking availability across Singapore. We curated the data from website at a 15-minute resolution spanning from January 1, 2025, to June 1, 2025, to capture high-frequency urban parking utilization patterns.

¹<https://toolkit.solcast.com.au/>

Following filtering and preprocessing, the final dataset includes 354 storey carparks. We use the last one week data as test set.

Finland Traffic This dataset comprises real-time traffic volume measurements sourced from Digitraffic platform. The data is acquired from fixed monitoring stations positioned throughout the Finnish road network. The observational period spans from January 1, 2024, to January 1, 2025. To capture fine-grained temporal dynamics, the raw traffic counts were aggregated into a 15-minute resolution, providing a granular representation of traffic flow intensity and congestion patterns at specific road junctions.

Port Activity This dataset offers a high-resolution view of global maritime trade by tracking daily port activities and cargo estimates provided by the IMF. It encompasses diverse vessel types and trade volumes across multiple geographic regions. In addition to the original daily records, a weekly aggregated version is also generated for longitudinal analysis.

B.4. Health Care

ECDC COVID This dataset captures the daily dynamics of healthcare utilization sourced from the European Centre for Disease Prevention and Control (ECDC). It features time-series observations of daily hospital occupancy, defined as the total number of COVID-19 patients occupying hospital beds on a given day. The dataset covers a comprehensive period from January 5, 2020, to November 26, 2023, across multiple European regions.

Global Influenza This data is curated from FluNet, a global web-based platform for influenza virological surveillance, maintained by the WHO's GISRS network since 1997. It provides weekly-updated, country-level data on influenza subtypes. We select 15 representative countries and regions including the USA, UK, India, and Singapore for this dataset.

B.5. Finance

Crypto This dataset comprises daily price records for four major cryptocurrencies—Bitcoin, Ethereum, Litecoin, and Bitcoin Cash—covering the period from December 20, 2017, to September 30, 2025. Data from the final nine months of 2025 are designated as the test set to evaluate model generalizability.

US Term Structure This dataset tracks daily term premiums and instantaneous forward rates derived from the Kim and Wright (2005) arbitrage-free model. The data spans from January 2, 1990, to September 30, 2025, on a business-day frequency. We use data from the years 2024 and 2025 as the test set.

Oil Price This dataset records the daily trading prices of key energy commodities, specifically Crude Oil and various Refined Products. The data covers a business-day frequency from June 14, 2006, to September 30, 2025. Same as above, the observations from the year 2025 are reserved as the test set.

B.6. Economics

Job Claims This dataset tracks two key indicators of the U.S. labor market, specifically the 4-week moving averages of Initial Claims and Continued Claims. Sampled on a weekly basis, the data spans from January 1, 2022, to September 27, 2025. The final 52 weeks of the series are reserved as the test set.

Uncertainty-1M This multivariate dataset comprises three key monthly uncertainty indices of US—macroeconomic, financial, and real uncertainty, sourced from the JLN and LMN frameworks (Jurado et al., 2015; Ludvigson et al., 2021). These series quantify the 1-month-ahead unpredictability of the economic state, derived from a broad spectrum of real time series. The dataset covers the period from July 1960 to June 2025. We designate the data from January 2022 to June 2025 as test set.

Housing Inventory This dataset tracks monthly supply-side dynamics of the U.S. real estate market. It includes four key indicators: Active Listing Count, Median Days on Market, Median Listing Price per Square Foot, and Median Home Size. The data spans from July 2016 to December 2025.

JOLTS Sourced from the U.S. Bureau of Labor Statistics, Job Openings and Labor Turnover Survey (JOLTS) provides a comprehensive view of labor market dynamics. The dataset tracks monthly indicators such as Job Openings, Hires, and Quits, covering the period from December 2000 to August 2025.

US Labor This dataset provides a comprehensive overview of the U.S. labor market, aggregating monthly statistics on labor force participation, employment levels, and unemployment rates. The data spans from January 1994 to August 2025.

Vehicle Supply This dataset monitors supply-side dynamics in the U.S. automotive industry. It encompasses key metrics including domestic production, inventory levels, the inventory-to-sales ratio, and cross-border trade flows (imports from Canada/Mexico and exports). The data spans monthly from January 1993 to July 2025.

Auto Production-SF This dataset contains the regular seasonal adjustment factors for U.S. auto production. These statistical components represent recurring temporal patterns driven by annual events such as model changeovers and holiday shutdowns. The data covers the period from January 1996 to July 2026.

Commodity Production This dataset is a collection of historical monthly univariate time series tracking U.S. commodity production (e.g. steel, silver, etc). The series vary in length and predominantly cover the industrial dynamics of the early to mid-20th century

Commodity Import Similar to Commodity Production, this dataset includes historical monthly univariate time series of U.S. commodity import, including banana, coffee, crude rubber, etc.

WUI-Global This dataset includes quarterly World Uncertainty Indices (WUI) for 15 countries. The dataset spans from Q1 1952 to Q2 2025. We forecast the future 4 quarters (1 year), using the final 5 years as the test set.

Global Price This dataset tracks quarterly global market prices for a broad spectrum of commodities. It encompasses three major sectors: Energy (e.g., Crude Oil, Coal, Natural Gas), Metals (e.g., Aluminum, Copper, Iron Ore), and Agriculture (e.g., Coffee, Soybeans, Wheat). Additionally, it features aggregate indices for food, beverages, and industrial materials. The data spans from 1990 Q1 to 2025 Q2.

B.7. Sales

Vehicle Sales This dataset encompasses monthly U.S. vehicle sales across diverse categories from 1976 through 2025. Consistent with our experimental setup, the final five-year period is reserved as a hold-out test set.

Online Retail II This dataset encompasses all transactions for a UK-based, non-store online retailer from December 1, 2009, to December 9, 2011. We aggregate individual transactions into daily totals to derive a univariate time series representing the total daily sales volume.

Supply Chain (Customer & Location) This dataset comprises five years of simulated delivery records spanning from January 2, 2020, to June 30, 2025. To capture both micro and macro demand patterns, the raw transactional data—including daily order counts, piece volumes, and total revenue—are aggregated into two distinct multivariate time series. The customer-level version treats each individual client as a separate variate, while the location-level version aggregates these metrics by geographic city. This dual-aggregation approach allows for a comprehensive analysis of supply chain dynamics from both relational and spatial perspectives.

B.8. CloudOPS

Azure2019 Following the methodology of (Woo et al., 2023), we curated and processed CPU utilization traces from the Azure cloud platform. The dataset captures average, minimum, and maximum CPU metrics at a 5-minute resolution across three workload categories: Delay-insensitive (D), Interactive (I), and Unknown (U), where categories D and I exhibit longer temporal durations compared to U. Due to the vast volume of raw data, we randomly sampled 2,000 instances; after applying quality filters, a refined subset was retained, comprising 989 instances for D, 492 for I, and 78 for U.

B.9. Industry

Smart Manufacturing Designed for predictive maintenance and anomaly detection, this dataset simulates IoT sensor readings from industrial machinery. Due to the inherent irregular sampling rate of the raw logs, we downsample the series to an hourly level. The dataset tracks five multivariate features critical to machine health: temperature, vibration, humidity, pressure, and energy consumption.

MetroPT-3 This dataset comprises multivariate time series recorded from the Air Production Unit (APU) of a metro train's compressor between February and August 2020. Sourced from an operational environment, the original data captures 15 distinct signals—including pressure, motor current, oil temperature, and valve states—logged at a frequency of 1Hz. We downsample the data into 5-minute resolution for practical predictive maintenance purposes.

C. Implementation Details

C.1. Data Screening Pipeline

As described in Section 4.2, we implemented an automated quality assurance pipeline to ensure the data integrity of the time series in our benchmark. It systematically examines each series at both the variate and dataset levels. The pipeline operates in four phases, as outlined in Algorithm 1. For each variate, we apply a set of rules to assess data quality and impute extreme outliers during the screening process. The detailed variate-level checks are presented in Algorithm 2.

The pipeline outputs a comprehensive quality summary \mathcal{Q} that documents all check results, along with a cleaned dataset \mathcal{D}' where extreme outliers have been imputed via forward-filling. These outputs are then passed to the subsequent human decision-making stage for data finalization and task formulation.

Algorithm 1 Time Series Quality Assurance Pipeline

Require: Dataset $\mathcal{D} = \{\mathbf{X}^{(i)}\}_{i=1}^N$ where each $\mathbf{X}^{(i)} \in \mathbb{R}^{L_i \times D_i}$
Require: Parameters: τ_{miss} (missing rate threshold), τ_{corr} (correlation threshold), $\tau_{\text{len}}^{(f)}$ (minimum length per frequency f)
Ensure: Quality summary \mathcal{Q} and cleaned dataset \mathcal{D}'

```

1: Phase 1: Per-Series Processing
2: for each series  $\mathbf{X}^{(i)} \in \mathcal{D}$  do
3:   Normalize timestamp column to first position
4:    $f \leftarrow \text{INFERFREQUENCY}(\mathbf{X}^{(i)})$ 
5:    $\tau_{\text{len}} \leftarrow \tau_{\text{len}}^{(f)}$ 
6:   Fill missing timestamps via reindexing with  $f$ 
7: Phase 2: Per-Variate Quality Checks
8: for each variate  $\mathbf{x}_d \in \mathbf{X}^{(i)}$ ,  $d = 1, \dots, D_i$  do
9:    $\text{quality}_d \leftarrow \text{UNIVARIATEQUALITYCHECK}(\mathbf{x}_d, \tau_{\text{miss}}, \tau_{\text{len}})$ 
10:  end for
11: Phase 3: Multivariate Correlation Check
12: if  $D_i > 1$  then
13:   Compute Pearson correlation matrix  $\mathbf{R} \in \mathbb{R}^{D_i \times D_i}$ 
14:   Identify pairs  $(\mathbf{x}_j, \mathbf{x}_k)$  where  $|r_{jk}| > \tau_{\text{corr}}$ 
15: end if
16: end for
17: Phase 4: Cross-Series Correlation (for univariate datasets)
18: if all  $D_i = 1$  and all  $L_i$  equal then
19:   Compute inter-series correlation matrix
20:   Flag highly correlated series pairs
21: end if
22: return Quality summary  $\mathcal{Q}$ , cleaned dataset  $\mathcal{D}'$ 

```

Algorithm 2 Univariate Quality Check

Require: Variate $\mathbf{x} = (x_1, x_2, \dots, x_L) \in \mathbb{R}^L$, thresholds $\tau_{\text{miss}}, \tau_{\text{len}}$
Ensure: Quality result $\mathcal{R} = \{\text{predictable}, \tilde{\mathbf{x}}\}$

- 1: **Check 1: Data Type**
- 2: **if** \mathbf{x} is not numeric **then**
- 3: **return** $\{\text{predictable} = \text{False}\}$
- 4: **end if**
- 5: **Check 2: Data Integrity**
- 6: **if** $L < \tau_{\text{len}}$ **then**
- 7: predictable $\leftarrow \text{False}$
- 8: **end if**
- 9: $\rho_{\text{miss}} \leftarrow |\{t : x_t = \text{NaN}\}|/L$
- 10: **if** $\rho_{\text{miss}} > \tau_{\text{miss}}$ **then**
- 11: predictable $\leftarrow \text{False}$
- 12: **end if**
- 13: $\tilde{\mathbf{x}} \leftarrow \text{Forward-fill then backward-fill NaN values}$
- 14: **Check 3: Signal Existence (Constant Series Detection)**
- 15: $\text{topk_dom} \leftarrow \sum_{i=1}^5 p_{(i)}$ {Top-5 value frequencies}
- 16: $H \leftarrow -\sum_v p_v \log p_v / \log(|\mathcal{V}|)$ {Normalized entropy}
- 17: **if** $\text{topk_dom} \geq 0.5$ **or** $H < 0.1$ **then**
- 18: **return** $\{\text{predictable} = \text{False}\}$
- 19: **end if**
- 20: **Check 4: White Noise Test (Ljung-Box)**
- 21: $p_{\text{LB}} \leftarrow \text{LJUNGBOTEST}(\tilde{\mathbf{x}}, \text{lags} = [10, 20])$
- 22: **if** $\min(p_{\text{LB}}) > 0.05$ **then**
- 23: **return** $\{\text{predictable} = \text{False}\}$ {White Noise}
- 24: **end if**
- 25: **Check 5: Outlier Detection and Cleaning (Sliding Window IQR)**
- 26: **for** $t = 1$ to L **do**
- 27: $m_t \leftarrow \text{median}(\mathcal{W}_t)$, $\text{IQR}_t \leftarrow Q_{0.75}(\mathcal{W}_t) - Q_{0.25}(\mathcal{W}_t)$
- 28: $d_t \leftarrow |x_t - m_t|/\text{IQR}_t$
- 29: **end for**
- 30: $\mathcal{I}_{\text{trans}} \leftarrow \{t : k_{\text{trans}} < d_t < k_{\text{ext}}\}$, $\mathcal{I}_{\text{ext}} \leftarrow \{t : d_t \geq k_{\text{ext}}\}$
- 31: **if** $|\mathcal{I}_{\text{ext}}|/L > \tau_{\text{ext}}$ **then**
- 32: **return** $\{\text{predictable} = \text{False}\}$
- 33: **end if**
- 34: $\tilde{\mathbf{x}} \leftarrow \text{Replace } x_t \text{ for } t \in \mathcal{I}_{\text{ext}} \text{ with forward-filled values}$
- 35: **return** $\{\text{predictable} = \text{True}, \tilde{\mathbf{x}}\}$

C.2. Models

We evaluate 12 time series foundation models using their official checkpoints from HuggingFace. Table 3 summarizes the key hyperparameters used in our evaluation. All models are evaluated in a zero-shot setting without any fine-tuning. Experiments are run on a single NVIDIA RTX 3090 GPU (24GB VRAM).

Output Types. Models with quantile output produce 9 quantile forecasts at levels $\{0.1, 0.2, \dots, 0.9\}$. Models with sample-based output generate 100 Monte Carlo samples for probabilistic forecasting.

Multivariate Handling. Chronos2, VisionTS++, Toto, and Moirai (1.1) natively support multivariate time series input. For univariate models, we flatten multivariate series into independent univariate sequences and forecast each variate separately. For Moirai (1.1), when GPU memory is insufficient for multivariate inference, the model automatically falls back to univariate mode to complete the evaluation.

Table 3. Model configurations used in evaluation. Context length refers to the maximum number of historical time steps used as input. Input mode indicates whether the model natively supports multivariate time series or processes each variate independently (univariate). Output type specifies whether models produce quantile forecasts or sample-based probabilistic forecasts.

Model	Checkpoint	Context Length	Input Mode	Output Type
TimesFM 2.5	google/timesfm-2.5-200m-pytorch	4096	Univariate	Quantile
Chronos2	amazon/chronos-2	4000	Multivariate	Quantile
Kairos	mldi-lab/Kairos_50m	2048	Univariate	Quantile
Moirai 2.0	Salesforce/moirai-2.0-R-base	4000	Univariate	Quantile
VisionTS++	Lefei/VisionTSpp	4000	Multivariate	Quantile
TiRex	NX-AI/TiRex	2048	Univariate	Quantile
Toto	Datadog/Toto-Open-Base-1.0	4096	Multivariate	Sample (100)
Sundial	thumt/sundial-base-128m	2880	Univariate	Sample (100)
TimesFM 2.0	google/timesfm-2.0-500m-pytorch	2048	Univariate	Quantile
Chronos-bolt	amazon/chronos-bolt-base	4000	Univariate	Quantile
Moirai	Salesforce/moirai-1.1-R-base	4000	Multivariate	Sample (100)
TimesFM 1.0	google/timesfm-1.0-200m-pytorch	512	Univariate	Quantile

C.3. Metrics

Mean Absolute Scaled Error (MASE). MASE provides a scale-independent assessment of forecast accuracy by normalizing the prediction error against the mean absolute error of a seasonal naive baseline. This normalization ensures interpretability across variates with varying magnitudes. It is defined as:

$$\text{MASE} = \frac{1}{H} \sum_{i=1}^H \frac{|\mathbf{Y}_i - \hat{\mathbf{Y}}_i|}{\frac{1}{H-s} \sum_{j=s+1}^H |\mathbf{Y}_j - \mathbf{Y}_{j-s}|},$$

where s denotes the periodicity of the data (e.g., season length), and H represents the forecasting horizon. $\mathbf{Y}, \hat{\mathbf{Y}} \in \mathbb{R}^{H \times D}$ denote the ground truth and the predicted values, respectively, over D dimensions. The term \mathbf{Y}_i refers to the value at the i -th future time step.

Continuous Ranked Probability Score (CRPS) To evaluate the quality of the predicted distribution, we employ CRPS, which measures the compatibility between the predicted cumulative distribution function (CDF) F and the observed ground truth \mathbf{Y} . The integral form is given by:

$$\text{CRPS}(F, \mathbf{Y}) = \int_0^1 2\Lambda_\alpha(F^{-1}(\alpha), \mathbf{Y}) d\alpha,$$

$$\Lambda_\alpha(q, \mathbf{Y}) = (\alpha - \mathbb{1}(\mathbf{Y} < q))(\mathbf{Y} - q),$$

where Λ_α represents the quantile loss (or pinball loss) at the quantile level α . To ensure computational tractability and provide a normalized metric for cross-dataset comparison, we utilize the normalized discrete approximation of CRPS. This is calculated as the average of the weighted Quantile Loss (wQL) across a set of discrete quantiles:

$$\text{CRPS} \approx \frac{1}{K} \sum_{k=1}^K \text{wQL}[\alpha_k],$$

$$\text{wQL}[\alpha] = 2 \frac{\sum_i \Lambda_\alpha(\hat{q}_i(\alpha), \mathbf{Y}_i)}{\sum_i |\mathbf{Y}_i|}.$$

Here, $\hat{q}_i(\alpha)$ denotes the predicted α -quantile at time step i . In our evaluation, we employ $K = 9$ equidistant quantiles, specifically $\alpha_k \in \{0.1, 0.2, \dots, 0.9\}$.

D. Time Series Features

D.1. Detailed Related Work

Early studies (Kang et al., 2017; Spiliotis et al., 2020) quantified statistical and meta-features—such as spectral entropy, trend and seasonality strength, seasonal period, ACF-1, kurtosis, skewness, non-linear autoregressive structure, and the optimal Box–Cox transformation parameter—primarily for PCA and dataset-level distribution visualization. Similarly, Monash (Godahewa et al., 2021) utilized ACF-1, trend and seasonality strength, entropy, and the Box–Cox parameter (λ) for distribution visualization. GIFT-EVAL (Aksu et al., 2024) characterized the most recent 500 time steps to reflect three temporal dimension: forecastability (trend and seasonal strength), regularity (entropy and Hurst exponent), and variability (stability and lumpiness). TFB (Qiu et al., 2024) expanded this scope by considering stationarity (via the modified Augmented Dick–Fuller test), correlation, and custom-defined metrics for shifting and transition. More recently, ProbTS (Zhang et al., 2024) analyzed trend, seasonality, and distribution complexity within fixed-length windows, while Boom (Cohen et al., 2025) selected six key features—including first-lag ACF, ARCH-LM statistic, spectral entropy, KPSS statistic, flat spots, and skewness—to characterize individual variates.

Despite this extensive characterization, prior works primarily utilize these features for data coverage analysis, visualization, and comparing distributional divergence against other benchmarks. Few studies adopt feature patterns as a distinct evaluation perspective. While TFB employs a single representative dataset per feature to reflect model performance, it lacks a systematic cross-dataset evaluation rooted in specific feature patterns.

In this work, we firstly introduce the pattern-driven analysis for cross-dataset evaluation. By archiving the pattern vector of each variate, we can use the pattern coding of a target pattern to retrieve variates exhibiting specific characteristics. The resulting aggregated metrics provide generalizable and high-level insights into model performance regarding each specific pattern.

D.2. Definition of Selected Feature

In this section, we provide detailed definitions and mathematical formulations for each structural time series feature described in Section 5.1. Consistent with the main text, we use $\mathbf{x} \in \mathbb{R}^L$ to represent a time series variate (e.g. a UTS) of length L . Our feature extraction is implemented based on the `tsfeatures` library (Garza et al., 2022). By default, we use the test split to compute the `tsfeatures` for the variate. However, for variates with a test length below 500, the full variate is used instead.

The computation of structural features ($F_1 - F_5$) relies on Seasonal and Trend decomposition using Loess (STL) (Cleveland et al., 1990). While the underlying implementation extends standard STL to handle multiple seasonalities, we configure the decomposition to focus on the dominant seasonal period to ensure consistent feature comparability across diverse datasets.

Accordingly, as shown in Equation 1, we decompose the variate \mathbf{x} into three additive component vectors:

- T (Trend) represents the smoothed trend-cycle component, estimated via a Loess smoother.
- S (Seasonality) corresponds to the periodic seasonal component.
- R (Remainder) denotes the residual component, capturing the variability not explained by the trend or seasonality.

Based on this decomposition, the computation of our structural time series features is defined as follows.

Trend Strength (F_1) This feature quantifies the strength of the trend component relative to the remainder. It is computed as:

$$F_1 = \max \left(0, 1 - \frac{\text{Var}(R)}{\text{Var}(T + R)} \right) \quad (3)$$

where $\text{Var}(\cdot)$ denotes the variance. A value close to 1 indicates that the trend variance dominates the remainder variance, signifying a strong trend, while a value close to 0 implies the trend is negligible compared to the noise.

Trend Linearity (F_2) To characterize the structural shape of the trend, we fit an orthogonal quadratic regression model to the estimated trend component T :

$$T_t = \beta_0 + \beta_1 P_1(t) + \beta_2 P_2(t) + \varepsilon_t, \quad \text{for } t = 1, \dots, L \quad (4)$$

where P_1 and P_2 are the first-order (linear) and second-order (quadratic) orthogonal polynomials of the time index, respectively. Trend Linearity (F_2) is defined as the coefficient of the linear term:

$$F_2 = \beta_1 \quad (5)$$

This metric captures the overall direction and steepness of the linear progression within the trend, independent of any curvature effects due to the orthogonality of the regressors.

Seasonality Strength (F_3) Analogous to Trend Strength, this feature quantifies the relative importance of the seasonal component compared to the noise. It is computed as:

$$F_3 = \max \left(0, 1 - \frac{\text{Var}(R)}{\text{Var}(S + R)} \right) \quad (6)$$

A value close to 1 implies that the seasonal variation is much larger than the residual variability, indicating a distinct and strong seasonal pattern.

Seasonality Correlation (F_4) This feature measures the stability and consistency of the seasonal shape across different cycles. Let m be the seasonal period. We first truncate the seasonal component S to contain only full cycles and reshape it into $K = \lfloor L/m \rfloor$ segments, denoted as vectors $\mathbf{s}_1, \dots, \mathbf{s}_K \in \mathbb{R}^m$. F_4 is defined as the average Pearson correlation coefficient between all pairs of seasonal cycles:

$$F_4 = \frac{2}{K(K-1)} \sum_{i=1}^K \sum_{j=i+1}^K \text{Corr}(\mathbf{s}_i, \mathbf{s}_j) \quad (7)$$

High values indicate that the seasonal pattern repeats with a consistent shape over time, while low values suggest an evolving or unstable seasonal structure.

Residual ACF-1 (F_5) This feature captures the linear dependence between consecutive values in the remainder component. It is calculated as the first-order autocorrelation coefficient:

$$F_5 = \text{Corr}(R_t, R_{t-1}) = \frac{\sum_{t=2}^L (R_t - \bar{R})(R_{t-1} - \bar{R})}{\sum_{t=1}^L (R_t - \bar{R})^2} \quad (8)$$

where \bar{R} is the mean of the remainder vector. A value significantly different from zero suggests that there is still temporal structure (information) left in the residuals that was not captured by the trend or seasonality components.

Complexity (F_6) This global feature quantifies the overall forecast difficulty of the raw variate \mathbf{x} . Similar to F_6 , it is computed using the spectral entropy of the original time series:

$$F_6 = - \int_{-\pi}^{\pi} \hat{f}_{\mathbf{x}}(\lambda) \log \hat{f}_{\mathbf{x}}(\lambda) d\lambda \quad (9)$$

where $\hat{f}_{\mathbf{x}}(\lambda)$ is the normalized spectral density of \mathbf{x} . Higher complexity values indicate a series with high entropy (more noise-like), suggesting greater difficulty in forecasting.

Stationarity (F_7) This binary feature indicates whether the raw time series \mathbf{x} is stationary. It is derived from the Augmented Dickey-Fuller (ADF) unit root test (Dickey & Fuller, 1979). Let p_{ADF} be the p-value obtained from the test. The feature is defined as:

$$F_7 = \mathbb{I}(p_{\text{ADF}} < 0.05) \quad (10)$$

where $\mathbb{I}(\cdot)$ is the indicator function. $F_7 = 1$ implies the series is stationary (no unit root) with 95% confidence, whereas $F_7 = 0$ indicates non-stationarity.

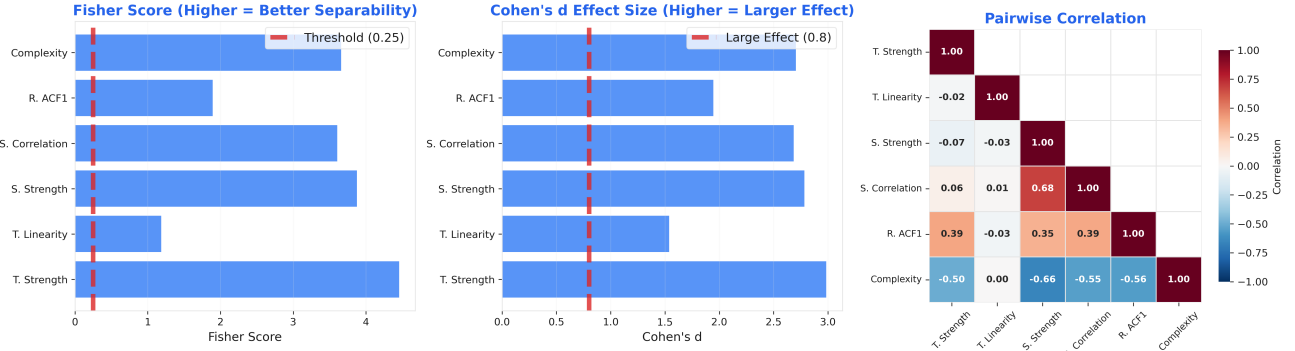


Figure 7. Quantitative analysis of feature informativeness for median-based binary grouping. **Left:** Fisher Score measures the ratio of between-group to within-group variance; all features exceed the threshold of 0.25 (red dashed line), indicating strong discriminative power. **Middle:** Cohen's d quantifies effect size; all features surpass the large effect threshold of 0.8 (red dashed line), with values ranging from 1.54 to 2.98. **Right:** Pairwise correlation matrix shows that most features exhibit low to moderate correlations ($|r| < 0.7$), confirming they capture complementary time series characteristics

D.3. Feature Distribution Analysis

To validate the effectiveness of median-based binary grouping for time series characterization, we conduct a quantitative analysis of the selected features. Our goal is to demonstrate that each feature provides meaningful discriminative power when partitioning time series into two groups based on its median value. Specifically, we aim to show that the resulting groups are statistically distinct, justifying the use of these features for stratified evaluation and analysis.

We employ two complementary metrics: **Fisher Score** for measuring class separability, and **Cohen's d** for quantifying effect size. Together, these metrics provide both a variance-normalized measure of group separation and an interpretable standardized effect size.

Fisher Score. The Fisher Score is a classical feature selection criterion that measures the ratio of between-class variance to within-class variance. For a feature F_k with two groups defined by a threshold (median), the Fisher Score is computed as:

$$\text{Fisher Score} = \frac{(\mu_1 - \mu_2)^2}{\sigma_1^2 + \sigma_2^2} \quad (11)$$

where μ_1, μ_2 are the means and σ_1^2, σ_2^2 are the variances of the two groups, respectively. A higher Fisher Score indicates better separability between groups. Following common practice in feature selection literature, we consider a Fisher Score > 0.25 as indicative of meaningful discriminative power.

Cohen's d . Cohen's d is a widely-used standardized effect size measure that quantifies the magnitude of difference between two group means in units of pooled standard deviation:

$$\text{Cohen's } d = \frac{\mu_1 - \mu_2}{\sigma_{\text{pooled}}} \quad (12)$$

where the pooled standard deviation is:

$$\sigma_{\text{pooled}} = \sqrt{\frac{(n_1 - 1)\sigma_1^2 + (n_2 - 1)\sigma_2^2}{n_1 + n_2 - 2}} \quad (13)$$

Cohen's d provides interpretable benchmarks: $|d| < 0.2$ indicates a small effect, $0.2 \leq |d| \leq 0.8$ a medium effect, and $|d| > 0.8$ a large effect (Cohen, 2013).

We analyze six features extracted from 6,625 time series variates across our benchmark. Figure 7 summarizes the quantitative results. Several key observations emerge from the analysis:

(1) All features demonstrate strong discriminative power. Every feature achieves a Fisher Score substantially above the 0.25 threshold, ranging from 1.19 (Trend Linearity) to 4.46 (Trend Strength). This confirms that median-based partitioning creates groups with meaningfully different distributions for each feature.

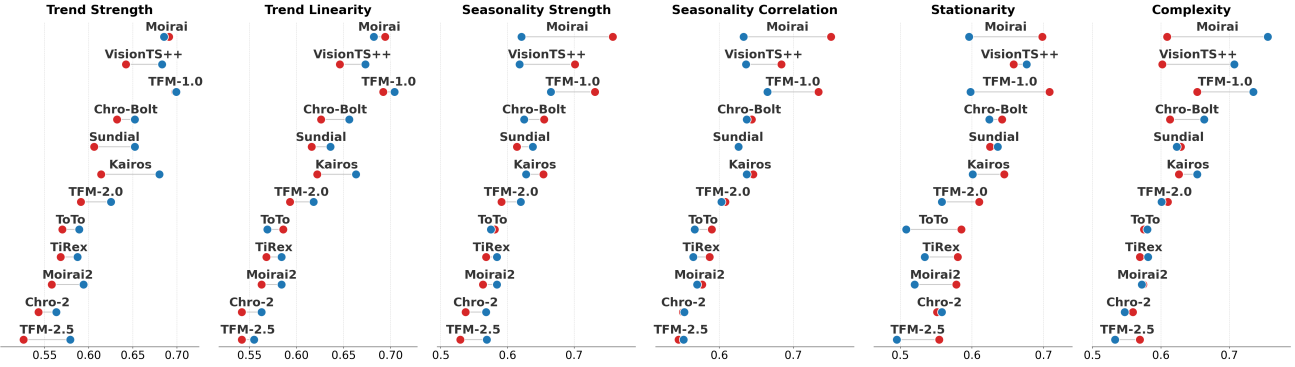


Figure 8. Comparison of CRPS across different feature-specific variates. Each row represents a model's performance on variates with $F_k = 1$ (red) and $F_k = 0$ (blue). The distance between dots indicates the performance difference of the model to that specific feature.

(2) Effect sizes are uniformly large. All features exhibit Cohen's d values well above 0.8, with the minimum being 1.54 (Trend Linearity) and the maximum reaching 2.98 (Trend Strength). According to standard interpretation guidelines, these represent *very large* effect sizes, indicating substantial practical differences between the high and low groups.

(3) Features capture complementary information. The pairwise correlation analysis reveals that most features exhibit low to moderate correlations ($|r| < 0.7$), indicating they capture distinct aspects of time series characteristics. Notably, Trend Linearity shows near-zero correlation with all other features ($|r| \leq 0.03$), confirming it measures an independent property. The strongest correlation occurs between Seasonality Strength and Seasonality Correlation ($r = 0.68$), which is expected as both characterize seasonal patterns. Complexity shows moderate negative correlations with seasonality-related features ($r = -0.66$ with Seasonality Strength, $r = -0.55$ with Seasonality Correlation) and Residual ACF1 ($r = -0.56$), suggesting that more complex time series tend to exhibit weaker seasonal patterns and lower residual autocorrelation. Overall, the correlation structure confirms that our feature set provides a diverse and complementary characterization of time series properties.

(4) Statistical significance. Mann-Whitney U tests confirm that all median-based groupings produce statistically significant differences ($p < 0.001$ for all features), ruling out the possibility that observed separations are due to chance.

These results validate our feature selection and demonstrate that median-based binary grouping produces meaningful stratifications of time series data. The consistently large effect sizes across all features support the use of this approach for analyzing model performance across different time series characteristics.

E. Full Results

This section presents the comprehensive numerical results of our experiments. We begin with the overall aggregated performance in Table 4, followed by a detailed pattern-level breakdown in Figure 8 and Table 5. Finally, we provide the granular dataset-level results for all 50 datasets in Table 6. To ensure a multifaceted evaluation, we report six metrics in total. For both MASE and CRPS, we provide the raw values, scores normalized by the Seasonal Naive baseline, and task-level rankings.

Table 4. Detailed overall performance of TSFMs on TIME benchmark. Task-level results are normalized by Seasonal Naive and aggregated via geometric mean. **Bold** indicates the best performance, and underlined indicates the second best.

Metric	TimesFM 2.5	Chronos2	Kairos	Moirai 2.0	VisionTS++	TiRex	ToTo	Sundial	TimesFM 2.0	Chronos-bolt	Moirai	TimesFM 1.0
MASE	0.667	0.712	0.738	0.701	0.803	0.697	<u>0.696</u>	0.755	0.717	0.784	0.823	0.787
CRPS	<u>0.559</u>	0.551	0.635	0.580	0.664	0.581	0.576	0.654	0.613	0.621	0.657	0.679
MASE Rank	3.10	<u>4.58</u>	7.86	5.86	9.57	4.72	<u>5.76</u>	8.32	6.88	9.18	10.85	10.45
CRPS Rank	<u>3.43</u>	2.67	9.37	5.71	9.30	4.65	5.43	10.74	7.55	8.27	9.87	11.34

Table 5. Pattern-specific performance (Normalized MASE and CRPS). Comparison between variates exhibiting a specific pattern ($=1$) and those that do not ($=0$).

Feature	Group	Metric	TimesFM 2.5	Chronos2	Kairos	Moirai 2.0	VisionTS++	TiReX	Toto	Sundial	TimesFM 2.0	Chronos-bolt	Moirai	TimesFM 1.0
Trend	$F_k = 1$	MASE	0.601	0.618	0.678	0.633	0.725	0.642	0.651	0.66	0.653	0.707	0.788	0.759
		CRPS	0.526	0.543	0.614	0.558	0.642	0.568	0.57	0.606	0.591	0.632	0.691	0.698
T. Linearity	$F_k = 1$	MASE	0.651	0.639	0.724	0.665	0.767	0.67	0.669	0.697	0.677	0.723	0.769	0.734
		CRPS	0.579	0.563	0.68	0.594	0.683	0.587	0.589	0.652	0.625	0.652	0.685	0.699
S. Correlation	$F_k = 1$	MASE	0.613	0.613	0.677	0.633	0.726	0.645	0.666	0.664	0.649	0.696	0.783	0.741
		CRPS	0.542	0.542	0.622	0.563	0.646	0.568	0.586	0.616	0.593	0.626	0.694	0.692
S. Correlation	$F_k = 0$	MASE	0.632	0.642	0.721	0.661	0.761	0.664	0.651	0.687	0.679	0.733	0.776	0.756
		CRPS	0.555	0.563	0.663	0.584	0.673	0.584	0.569	0.636	0.618	0.656	0.682	0.704
Seasonality	$F_k = 1$	MASE	0.586	0.593	0.694	0.619	0.772	0.632	0.648	0.653	0.64	0.715	0.843	0.766
		CRPS	0.529	0.537	0.654	0.563	0.701	0.568	0.581	0.614	0.591	0.655	0.758	0.731
R. ACF1	$F_k = 1$	MASE	0.662	0.664	0.702	0.676	0.713	0.679	0.67	0.7	0.689	0.713	0.717	0.73
		CRPS	0.569	0.568	0.628	0.584	0.618	0.584	0.575	0.638	0.62	0.625	0.621	0.665
Stationarity	$F_k = 1$	MASE	0.617	0.619	0.701	0.645	0.77	0.662	0.669	0.676	0.665	0.718	0.853	0.783
		CRPS	0.545	0.551	0.646	0.577	0.684	0.587	0.59	0.625	0.608	0.644	0.751	0.734
Complexity	$F_k = 1$	MASE	0.627	0.634	0.695	0.647	0.718	0.646	0.649	0.674	0.661	0.709	0.714	0.716
		CRPS	0.552	0.553	0.637	0.57	0.636	0.565	0.567	0.626	0.603	0.637	0.633	0.665

Table 6. Full results of Per Dataset.

Dataset	Metric	TimesFM 2.5	Chronos2	Kairos	Moirai 2.0	VisionTS++	TiReX	Toto	Sundial	TimesFM 2.0	Chronos-bolt	Moirai	TimesFM 1.0
Water Quality-Darwin	MASE (Raw)	0.993	1.089	1.220	1.092	1.270	1.024	1.007	1.292	1.182	1.214	1.428	1.098
	CRPS (Raw)	0.059	0.054	0.081	0.069	0.090	0.065	0.058	0.089	0.076	0.066	0.077	0.075
	MASE (Norm.)	0.739	0.839	0.928	0.816	0.989	0.766	0.754	0.953	0.888	0.932	1.072	0.827
	CRPS (Norm.)	0.504	0.466	0.694	0.584	0.795	0.553	0.500	0.745	0.645	0.565	0.675	0.630
	MASE (Rank)	1.667	4.667	10.333	4.667	9.667	3	2.333	10.333	8.667	9.333	12	5.333
Current Velocity/5T	MASE (Rank)	2.667	1	9.667	6.333	10.667	4.333	2.333	10.667	8.667	5	8.333	8.333
	MASE (Raw)	0.567	0.699	0.790	0.787	0.876	0.639	0.665	0.621	0.608	0.796	0.848	0.719
	CRPS (Raw)	0.276	0.283	0.343	0.315	0.293	0.278	0.289	0.291	0.314	0.319	0.289	0.361
	MASE (Norm.)	0.545	0.684	0.733	0.715	0.875	0.609	0.624	0.596	0.583	0.767	0.811	0.675
	CRPS (Norm.)	0.641	0.657	0.769	0.720	0.683	0.645	0.670	0.678	0.720	0.728	0.672	0.815
Current Velocity/10T	MASE (Rank)	1	6.667	10	9	10	4	4	4	3.667	2.667	9.667	10.667
	CRPS (Rank)	2	3.667	10	8	6.333	2	5.667	8	7	8.333	6.333	11.333
	MASE (Raw)	0.729	0.799	0.956	0.929	1.183	0.788	0.833	0.907	0.804	1.065	1.281	0.897
	CRPS (Raw)	0.277	0.270	0.337	0.326	0.367	0.284	0.296	0.320	0.306	0.334	0.386	0.329
	MASE (Norm.)	0.601	0.666	0.787	0.752	1.005	0.647	0.678	0.738	0.662	0.876	1.046	0.734
Current Velocity/15T	CRPS (Norm.)	0.649	0.633	0.786	0.757	0.862	0.666	0.691	0.749	0.712	0.779	0.903	0.766
	MASE (Rank)	1	4.333	8.667	7.667	11.333	2.333	4.333	6.667	4	10.667	12.333	6.333
	CRPS (Rank)	2	1	9.333	7.667	9.667	3	4.333	7	5.333	9	12	8
	MASE (Raw)	0.695	1.330	0.815	0.734	0.884	0.703	0.738	0.768	0.738	1.391	0.904	0.814
	CRPS (Raw)	0.333	0.332	0.354	0.342	0.358	0.333	0.343	0.360	0.350	0.343	0.363	0.364
Current Velocity/20T	MASE (Norm.)	0.648	1.264	0.754	0.682	0.840	0.654	0.685	0.714	0.685	1.319	0.836	0.752
	CRPS (Norm.)	0.659	0.655	0.697	0.675	0.708	0.658	0.677	0.710	0.689	0.678	0.716	0.717
	MASE (Rank)	1.333	12	8	4	8.667	1.667	4	6	4	13	9.667	7.667
	CRPS (Rank)	2.333	2	9	5.667	7.667	2	6	10	6.333	6.333	10.333	10.333
	MASE (Raw)	0.762	0.881	0.866	0.860	1.017	0.855	0.814	0.897	0.796	1.168	1.094	0.864
Current Velocity/H	CRPS (Raw)	0.316	0.305	0.350	0.339	0.368	0.391	0.324	0.338	0.329	0.430	0.367	0.355
	MASE (Norm.)	0.644	0.761	0.736	0.723	0.898	0.746	0.687	0.758	0.673	1.021	0.927	0.726
	CRPS (Norm.)	0.648	0.626	0.716	0.693	0.760	0.796	0.665	0.695	0.673	0.881	0.754	0.722
	MASE (Rank)	1	6.667	6.667	5.667	9.333	5	3.667	8.667	2.333	12.333	11.333	6.667
	CRPS (Rank)	2	1	8.667	6.333	7.667	6	4.667	7	4.667	10.667	10.333	9
CPHL/15T	MASE (Raw)	1.062	1.303	1.373	1.121	1.482	1.123	1.175	1.775	1.258	1.531	1.405	1.457
	CRPS (Raw)	0.308	0.304	0.374	0.323	0.363	0.305	0.325	0.330	0.359	0.355	0.355	0.409
	MASE (Norm.)	0.650	0.808	0.844	0.684	0.930	0.681	0.715	1.082	0.760	0.945	0.869	0.887
	CRPS (Norm.)	0.633	0.623	0.765	0.661	0.748	0.625	0.666	0.677	0.729	0.725	0.729	0.832
	MASE (Rank)	1.333	6.333	7.333	2.667	10	2	4	12.333	5.667	11	8	8.667
CPHL/15T	CRPS (Rank)	2.667	1.667	10	4	8.667	1.667	5	6.333	8.333	9	9	11.667
	MASE (Raw)	0.977	0.966	0.992	0.994	0.973	0.957	0.938	0.922	0.944	0.975	0.998	1.100
	CRPS (Raw)	0.213	0.215	0.225	0.216	0.213	0.213	0.208	0.216	0.212	0.217	0.222	0.252
	MASE (Norm.)	0.657	0.650	0.666	0.665	0.661	0.645	0.634	0.623	0.637	0.655	0.675	0.735
CPHL/15T	CRPS (Norm.)	0.615	0.618	0.647	0.620	0.622	0.614	0.601	0.626	0.611	0.624	0.643	0.724

Table 6. Full results of Per Dataset (Continued).

Dataset	Metric	TimesFM 2.5	Chronos2	Kairos	Moirai 2.0	VisionTS++	TiRex	Toto	Sundial	TimesFM 2.0	Chronos-bolt	Moirai	TimesFM 1.0
CPHL/30T	MASE (Rank)	7.667	4.667	10	7.333	7.333	4.333	3.667	1.333	4	4.667	6	11.667
	CRPS (Rank)	5	5	10	5.333	5.333	4.667	3.333	6	4.667	7.333	9.333	12
	MASE (Raw)	1.406	1.383	1.482	1.499	1.490	1.437	1.432	1.451	1.451	1.452	1.583	1.515
	CRPS (Raw)	0.248	0.249	0.270	0.267	0.266	0.262	0.255	0.287	0.262	0.265	0.285	0.286
	MASE (Norm.)	0.765	0.752	0.805	0.816	0.808	0.781	0.779	0.789	0.790	0.789	0.862	0.822
	CRPS (Norm.)	0.689	0.691	0.748	0.740	0.737	0.727	0.709	0.796	0.727	0.733	0.789	0.792
CPHL/H	MASE (Rank)	2	1	9	9.667	8	4	3.667	6.333	6.333	6	12	10
	CRPS (Rank)	1.333	1.667	8.667	7.667	6.333	4.667	3.333	11.333	5.667	5.667	10.667	11
	MASE (Raw)	1.645	1.666	1.699	1.699	1.828	1.718	1.748	1.841	1.705	1.738	1.801	1.869
	CRPS (Raw)	0.282	0.292	0.312	0.303	0.315	0.300	0.302	0.351	0.308	0.315	0.312	0.353
	MASE (Norm.)	0.800	0.807	0.825	0.824	0.890	0.831	0.841	0.888	0.827	0.843	0.875	0.900
	CRPS (Norm.)	0.743	0.766	0.815	0.795	0.829	0.785	0.791	0.916	0.805	0.826	0.820	0.918
Coastal T-S/5T	MASE (Rank)	1.667	1.667	4.333	5	10	5.333	6	10.333	5.333	7.333	9.667	11.333
	CRPS (Rank)	1	2	8	5.333	8.333	3.333	5	11.333	7	8	7.333	11.333
	MASE (Raw)	1.019	1.391	1.135	1.078	1.127	1.051	1.033	1.171	1.071	1.440	1.199	1.139
	CRPS (Raw)	0.043	0.042	0.055	0.043	0.046	0.042	0.044	0.057	0.054	0.049	0.045	0.056
	MASE (Norm.)	0.733	1.014	0.810	0.774	0.816	0.755	0.743	0.830	0.768	1.048	0.856	0.818
	CRPS (Norm.)	0.504	0.489	0.635	0.507	0.534	0.489	0.507	0.669	0.616	0.566	0.527	0.645
Coastal T-S/15T	MASE (Rank)	1	11.667	7.333	4.667	7.333	3	2	8.333	4.333	12.667	9.333	8
	CRPS (Rank)	4.333	1	10.333	4.333	7.333	2	4	10.667	8.667	8	6.333	11
	MASE (Raw)	1.261	1.576	1.263	1.277	1.299	1.259	1.303	1.272	1.284	1.563	1.322	1.291
	CRPS (Raw)	0.072	0.069	0.081	0.070	0.076	0.068	0.069	0.093	0.080	0.075	0.069	0.082
	MASE (Norm.)	0.819	1.026	0.821	0.830	0.846	0.818	0.845	0.827	0.834	1.019	0.858	0.839
	CRPS (Norm.)	0.666	0.631	0.742	0.641	0.700	0.628	0.634	0.857	0.725	0.692	0.637	0.750
Coastal T-S/20T	MASE (Rank)	1.667	12.333	3.333	5.333	7	2	8.667	4	6.333	12	9.333	7.333
	CRPS (Rank)	6.667	2.333	10	4.667	9.333	1.333	2.667	11.333	7.667	8	4	10
	MASE (Raw)	0.881	0.996	1.271	1.131	1.276	1.116	1.102	1.488	1.268	1.712	2.107	1.074
	CRPS (Raw)	0.004	0.004	0.006	0.005	0.006	0.006	0.005	0.006	0.005	0.009	0.011	0.005
	MASE (Norm.)	0.547	0.640	0.809	0.715	0.878	0.743	0.673	0.873	0.762	1.116	1.258	0.674
	CRPS (Norm.)	0.512	0.601	0.877	0.708	0.995	0.896	0.710	0.860	0.717	1.474	1.456	0.697
Coastal T-S/H	MASE (Rank)	1	3.333	8.667	6.333	7.333	5.667	4	9	7.333	11.667	12	4.667
	CRPS (Rank)	1	2.667	9.333	6	8	6	5.333	9.667	5.667	12.333	11.667	5
	MASE (Raw)	1.618	1.999	1.732	1.637	1.797	1.718	1.602	1.955	1.859	2.106	1.896	1.909
	CRPS (Raw)	0.029	0.030	0.033	0.030	0.033	0.031	0.029	0.034	0.035	0.031	0.033	0.038
	MASE (Norm.)	0.778	1.001	0.842	0.791	0.902	0.820	0.774	0.925	0.888	1.054	0.920	0.920
	CRPS (Norm.)	0.576	0.603	0.648	0.597	0.667	0.617	0.576	0.682	0.679	0.622	0.667	0.739
SG Weather	MASE (Rank)	2.333	9	5.667	3	6	4.333	2	10	7	12.333	8.667	9.333
	CRPS (Rank)	2	4.333	7.667	3.667	8	5	1.333	10.667	9	6	9.333	11
	MASE (Raw)	0.881	0.882	0.899	0.899	1.037	0.889	0.888	0.906	0.913	0.906	0.961	0.932
	CRPS (Raw)	0.177	0.176	0.181	0.185	0.215	0.178	0.178	0.200	0.188	0.187	0.201	0.196
	MASE (Norm.)	0.739	0.740	0.754	0.754	0.870	0.746	0.745	0.760	0.766	0.760	0.806	0.782
	CRPS (Norm.)	0.548	0.545	0.562	0.573	0.665	0.551	0.552	0.620	0.582	0.580	0.623	0.608
SG PM 2.5	MASE (Rank)	1.333	1.667	5.667	5.667	12	3.333	3.667	7	9	7.667	11	10
	CRPS (Rank)	1.667	1.333	5	6	12	3.333	3.667	10.333	7.667	7.333	10.667	9
	MASE (Raw)	0.935	0.915	0.920	0.937	0.933	0.919	0.927	0.920	0.926	0.948	0.946	0.978
	CRPS (Raw)	0.320	0.311	0.317	0.319	0.317	0.312	0.315	0.335	0.320	0.326	0.326	0.339
	MASE (Norm.)	0.750	0.734	0.738	0.752	0.749	0.738	0.744	0.738	0.743	0.760	0.758	0.784
	CRPS (Norm.)	0.694	0.674	0.687	0.692	0.688	0.676	0.682	0.727	0.693	0.708	0.706	0.736
NE China Wind	MASE (Rank)	7.667	2.667	3	8.667	6.333	2.667	6	3.333	6.333	10.333	9	12
	CRPS (Rank)	6.333	1.667	4	6.667	5.333	2.667	4.333	11	6	9	9.333	11.667
	MASE (Raw)	0.846	0.874	0.871	0.887	1.232	0.849	0.869	0.865	0.862	0.913	0.851	0.946
	CRPS (Raw)	0.414	0.414	0.431	0.428	0.556	0.414	0.411	0.431	0.420	0.426	0.425	0.460
	MASE (Norm.)	0.715	0.731	0.731	0.742	1.084	0.713	0.727	0.733	0.724	0.766	0.716	0.794
	CRPS (Norm.)	0.618	0.618	0.643	0.639	0.839	0.620	0.614	0.643	0.626	0.635	0.636	0.689
Australia Solar	MASE (Rank)	3.333	5.667	6	7.667	13	2	5.333	6.333	5	10	3.667	11
	CRPS (Rank)	3.667	3	8.333	8	12	4	2.333	8.333	4.333	6.333	6.667	11
	MASE (Raw)	0.606	0.599	0.594	0.620	0.560	0.584	0.604	0.625	0.650	0.581	0.666	0.663
	CRPS (Raw)	0.232	0.227	0.233	0.253	0.229	0.236	0.239	0.268	0.243	0.235	0.247	0.259
	MASE (Norm.)	0.854	0.844	0.837	0.873	0.789	0.823	0.851	0.881	0.916	0.818	0.939	0.934
	CRPS (Norm.)	0.741	0.726	0.746	0.811	0.732	0.753	0.763	0.858	0.775	0.754	0.793	0.829
EPF Electricity Price	MASE (Rank)	6.333	5.333	4.333	8	1.333	3.333	5.667	8.667	10	2.333	11.333	11.333
	CRPS (Rank)	3.333	2	4.333	10.333	2.333	5.333	6.667	12	7.333	5	8.667	10.667
	MASE (Raw)	1.221	1.193	1.272	1.207	1.474	1.163	1.229	1.206	1.232	1.235	1.243	1.289
	CRPS (Raw)	0.149	0.147	0.156	0.150	0.184	0.144	0.156	0.159	0.153	0.154	0.151	0.158
	MASE (Norm.)	0.688	0.671	0.715	0.678	0.836	0.655	0.692	0.680	0.693	0.694	0.701	0.726
	CRPS (Norm.)	0.637	0.630	0.665	0.643	0.793	0.618	0.671	0.683	0.654	0.656	0.647	0.677
OpenElectricity NEM	MASE (Rank)	5	2.333	10.333	4	12	1	6.667	4.667	6.333	6.667	8.333	10.667
	CRPS (Rank)	4	2	8.667	4	12	1	8	9.667	6.333	6.333	6.333	9.667
	MASE (Raw)	0.582	0.563	0.618	0.609	0.825	0.684	0.583	0.638	0.743	0.691	0.814	1.060
	CRPS (Raw)	0.174	0.160	0.191	0.183	0.240	0.185	0.165	0.193	0.186	0.183	0.205	0.238
	MASE (Norm.)	0.538	0.522	0.574	0.565	0.790	0.627	0.538	0.587	0.675	0.638	0.748	0.972
	CRPS (Norm.)	0.507	0.468	0.555	0.532	0.716	0.539	0.480	0.563	0.544	0.537	0.607	0.695
EWELD Load	MASE (Rank)	2.667	1	5.667	4.333	9.667	7.667	2.333	5.333	9	8	11	12.333
	CRPS (Rank)	3	1.333	7.667	5.667	9.333	6.333	1.667	9.333	6.667	5.667	9.667	12
	MASE (Raw)	0.667	0.650	0.686	0.677	0.776	0.653	0.696	0.667	0.669	0.675	0.853	0.994
	CRPS (Raw)	0.226	0.214	0.276	0.228	0.382	0.208	0.209	0.329	0.280	0.245	0.294	0.528
	MASE (Norm.)	0.673	0.654	0.695	0.682	0.789	0.660	0.702	0.673	0.678	0.680	0.864	1.009

Table 6. Full results of Per Dataset (Continued).

Dataset	Metric	TimesFM 2.5	Chronos2	Kairos	Moirai 2.0	VisionTS++	TiRex	Toto	Sundial	TimesFM 2.0	Chronos-bolt	Moirai	TimesFM 1.0
SG Carpark	CRPS (Norm.)	0.335	0.319	0.390	0.342	0.485	0.312	0.319	0.436	0.391	0.358	0.439	0.685
	MASE (Rank)	4.333	2.667	6.667	6	9.667	2	9	4	4.667	6	11	12.667
	CRPS (Rank)	3.667	2	6.667	6.333	10	1.667	5.333	9	6.333	5.333	9.667	12
	MASE (Raw)	0.579	0.537	0.625	0.588	0.644	0.634	0.804	0.597	0.635	0.648	1.021	0.923
	CRPS (Raw)	0.040	0.037	0.045	0.041	0.045	0.043	0.052	0.044	0.046	0.045	0.067	0.067
	MASE (Norm.)	0.520	0.484	0.566	0.527	0.591	0.568	0.678	0.532	0.569	0.569	0.936	0.818
Finland Traffic	CRPS (Norm.)	0.465	0.432	0.532	0.474	0.541	0.503	0.586	0.513	0.531	0.514	0.797	0.773
	MASE (Rank)	2.667	1	6.667	4	6.667	7.333	9.667	4	7	6.333	11.667	11.333
	CRPS (Rank)	2.333	1	8.333	3.333	6.667	5.667	9	6	7.333	5.667	11.333	11.333
	MASE (Raw)	0.522	0.505	0.540	0.525	0.560	0.607	0.594	0.563	0.596	0.559	0.895	0.639
	CRPS (Raw)	0.167	0.159	0.188	0.163	0.175	0.180	0.181	0.188	0.200	0.166	0.286	0.197
	MASE (Norm.)	0.555	0.536	0.576	0.558	0.600	0.647	0.633	0.590	0.636	0.595	0.946	0.682
Port Activity/D	CRPS (Norm.)	0.463	0.441	0.515	0.451	0.481	0.499	0.502	0.522	0.550	0.461	0.787	0.547
	MASE (Rank)	2.667	1	4.667	3.333	6	8.667	8	6	8.333	6.333	12.333	11
	CRPS (Rank)	3	1.333	7.333	3	5.333	7	6.667	8	10	4.333	12	10
	MASE (Raw)	0.660	0.659	0.663	0.660	0.666	0.661	0.665	0.675	0.662	0.662	0.667	0.663
	CRPS (Raw)	0.591	0.599	0.619	0.588	0.619	0.589	0.594	0.699	0.596	0.599	0.601	0.595
	MASE (Norm.)	0.575	0.574	0.578	0.575	0.580	0.576	0.580	0.589	0.577	0.577	0.581	0.578
Port Activity/W	CRPS (Norm.)	0.176	0.178	0.184	0.175	0.184	0.175	0.177	0.208	0.177	0.178	0.179	0.177
	MASE (Rank)	3	1	8	2	10	4	9	12	5	6	11	7
	CRPS (Rank)	3	7	10	1	11	2	4	12	6	8	9	5
	MASE (Raw)	0.770	0.779	0.785	0.771	0.773	0.778	0.787	0.800	0.765	0.784	0.788	0.794
	CRPS (Raw)	0.259	0.260	0.266	0.258	0.260	0.259	0.262	0.274	0.255	0.267	0.266	0.265
	MASE (Norm.)	0.748	0.757	0.763	0.749	0.751	0.755	0.764	0.777	0.742	0.761	0.765	0.771
ECDC COVID/D	CRPS (Norm.)	0.524	0.527	0.539	0.522	0.527	0.524	0.530	0.554	0.517	0.541	0.539	0.537
	MASE (Rank)	2	6	8	3	4	5	9	12	1	7	10	11
	CRPS (Rank)	3	6	10	2	5	4	7	12	1	11	9	8
	MASE (Raw)	3.364	3.225	3.943	3.392	3.441	3.006	3.061	3.176	3.423	3.359	4.267	3.643
	CRPS (Raw)	0.297	0.305	0.568	0.282	0.351	0.317	0.286	0.315	0.472	0.301	0.343	0.442
	MASE (Norm.)	0.940	0.902	1.102	0.948	0.962	0.840	0.856	0.888	0.957	0.939	1.193	1.018
ECDC COVID/W	CRPS (Norm.)	0.479	0.492	0.916	0.456	0.566	0.511	0.462	0.509	0.762	0.485	0.552	0.713
	MASE (Rank)	6	4	12	7	9	1	2	3	8	5	13	11
	CRPS (Rank)	3	5	12	1	9	7	2	6	11	4	8	10
	MASE (Raw)	1.426	1.488	2.337	1.470	1.451	1.232	1.501	1.302	1.884	1.354	1.633	2.250
	CRPS (Raw)	0.621	0.577	0.883	0.591	0.567	0.442	0.589	0.423	0.661	0.473	0.609	0.833
	MASE (Norm.)	0.878	0.916	1.439	0.905	0.893	0.759	0.924	0.801	1.160	0.833	1.005	1.385
Global Influenza	CRPS (Norm.)	0.780	0.725	1.110	0.743	0.713	0.556	0.740	0.532	0.831	0.594	0.765	1.047
	MASE (Rank)	4	7	13	6	5	1	8	2	11	3	10	12
	CRPS (Rank)	9	5	13	7	4	2	6	1	10	3	8	12
	MASE (Raw)	0.524	0.583	0.544	0.560	0.666	0.639	0.564	0.671	0.626	0.632	0.570	0.580
	CRPS (Raw)	0.374	0.363	0.395	0.344	0.684	0.401	0.396	0.429	0.467	0.452	0.348	0.425
	MASE (Norm.)	0.445	0.495	0.461	0.475	0.565	0.542	0.479	0.569	0.531	0.536	0.483	0.492
Crypto	CRPS (Norm.)	0.076	0.074	0.080	0.070	0.139	0.081	0.080	0.087	0.095	0.092	0.070	0.086
	MASE (Rank)	1	7	2	3	11	10	4	12	8	9	5	6
	CRPS (Rank)	4	3	5	1	12	7	6	9	11	10	2	8
	MASE (Raw)	5.706	5.674	7.074	5.713	8.826	5.465	6.080	5.714	5.900	6.025	6.304	6.364
	CRPS (Raw)	0.086	0.083	0.096	0.087	0.132	0.082	0.091	0.088	0.089	0.092	0.093	0.093
	MASE (Norm.)	1.005	1	1.246	1.006	1.555	0.963	1.071	1.007	1.039	1.061	1.111	1.121
US Term Structure	CRPS (Norm.)	0.887	0.853	0.981	0.889	1.351	0.842	0.934	0.909	0.915	0.946	0.952	0.952
	MASE (Rank)	4	2	12	5	13	1	9	6	7	8	10	11
	CRPS (Rank)	3	2	11	4	13	1	7	5	6	8	10	9
	MASE (Raw)	1.458	1.487	1.602	1.542	3.484	1.487	1.563	1.510	1.506	1.586	1.712	1.542
	CRPS (Raw)	0.210	0.209	0.224	0.215	0.406	0.208	0.221	0.218	0.214	0.227	0.212	0.218
	MASE (Norm.)	0.837	0.854	0.920	0.886	2.001	0.854	0.897	0.867	0.865	0.911	0.983	0.886
Oil Price	CRPS (Norm.)	0.846	0.840	0.903	0.865	1.634	0.837	0.889	0.876	0.863	0.912	0.853	0.876
	MASE (Rank)	1	2	10	6	13	3	8	5	4	9	11	7
	CRPS (Rank)	3	2	10	6	13	1	9	8	5	11	4	7
	MASE (Raw)	1.307	1.298	1.343	1.383	2.290	1.312	1.319	1.293	1.344	1.351	1.662	1.476
	CRPS (Raw)	0.045	0.045	0.046	0.047	0.088	0.045	0.045	0.046	0.046	0.046	0.057	0.050
	MASE (Norm.)	0.871	0.865	0.895	0.921	1.526	0.875	0.879	0.862	0.896	0.900	1.107	0.984
Job Claims	CRPS (Norm.)	0.836	0.836	0.862	0.882	1.651	0.840	0.849	0.869	0.854	0.863	1.070	0.939
	MASE (Rank)	3	8	10	4	7	9	1	13	6	12	2	11
	CRPS (Rank)	5	6	10	2	7	9	1	13	4	12	3	11
	MASE (Raw)	0.376	0.351	0.339	0.374	0.463	0.436	0.382	0.422	0.448	0.417	0.420	0.551
	CRPS (Raw)	0.031	0.027	0.028	0.029	0.040	0.033	0.028	0.035	0.038	0.033	0.032	0.043
	MASE (Norm.)	0.355	0.331	0.321	0.354	0.438	0.412	0.361	0.399	0.424	0.394	0.397	0.520
Uncertainty-1M	CRPS (Norm.)	0.392	0.343	0.356	0.363	0.505	0.415	0.356	0.443	0.473	0.414	0.402	0.546
	MASE (Rank)	4	2	1	3	11	9	5	8	10	6	7	12
	CRPS (Rank)	5	1	2	4	11	8	3	9	10	7	6	12
	MASE (Raw)	0.428	0.529	0.512	0.526	0.469	0.579	0.412	1.035	0.566	0.527	0.543	0.496
	CRPS (Raw)	0.043	0.053	0.047	0.044	0.045	0.058	0.042	0.100	0.052	0.054	0.049	0.055

Table 6. Full results of Per Dataset (Continued).

Dataset	Metric	TimesFM 2.5	Chronos2	Kairos	Moirai 2.0	VisionTS++	TiRex	Toto	Sundial	TimesFM 2.0	Chronos-bolt	Moirai	TimesFM 1.0
JOLTS	MASE (Norm.)	0.595	0.736	0.712	0.732	0.652	0.806	0.573	1.440	0.787	0.733	0.756	0.690
	CRPS (Norm.)	0.644	0.792	0.701	0.663	0.671	0.869	0.635	1.499	0.787	0.807	0.733	0.821
	MASE (Rank)	2	8	5	6	3	11	1	13	10	7	9	4
	CRPS (Rank)	2	8	5	3	4	11	1	13	7	9	6	10
	MASE (Raw)	1.017	0.906	1.244	1.041	1.205	1.040	1.071	1.546	1.109	1.056	1.501	1.480
	CRPS (Raw)	0.063	0.058	0.075	0.065	0.076	0.064	0.068	0.094	0.069	0.065	0.090	0.093
US Labor	MASE (Norm.)	0.622	0.555	0.761	0.637	0.738	0.637	0.656	0.946	0.679	0.647	0.919	0.906
	CRPS (Norm.)	0.628	0.572	0.742	0.642	0.750	0.640	0.672	0.931	0.682	0.645	0.897	0.924
	MASE (Rank)	2	1	9	4	8	3	6	12	7	5	11	10
	CRPS (Rank)	2	1	8	4	9	3	6	12	7	5	10	11
	MASE (Raw)	0.779	1.014	1.056	0.811	0.908	0.966	0.772	1.452	0.833	0.965	0.903	0.829
	CRPS (Raw)	0.042	0.057	0.060	0.046	0.053	0.049	0.044	0.062	0.045	0.056	0.055	0.044
Vehicle Supply	MASE (Norm.)	0.436	0.568	0.592	0.454	0.509	0.541	0.433	0.813	0.466	0.540	0.506	0.464
	CRPS (Norm.)	0.380	0.516	0.543	0.409	0.476	0.437	0.397	0.553	0.400	0.505	0.497	0.391
	MASE (Rank)	2	10	11	3	7	9	1	12	5	8	6	4
	CRPS (Rank)	1	10	11	5	7	6	3	12	4	9	8	2
	MASE (Raw)	0.798	0.708	0.884	0.757	1.137	0.694	0.764	0.717	0.710	0.813	0.791	0.973
	CRPS (Raw)	0.188	0.167	0.236	0.190	0.327	0.159	0.172	0.157	0.157	0.195	0.174	0.278
Auto Production-SF	MASE (Norm.)	0.719	0.638	0.796	0.682	1.024	0.625	0.688	0.646	0.639	0.732	0.712	0.877
	CRPS (Norm.)	0.541	0.481	0.679	0.546	0.941	0.458	0.496	0.452	0.452	0.561	0.501	0.800
	MASE (Rank)	8	2	10	5	13	1	6	4	3	9	7	11
	CRPS (Rank)	7	4	10	8	12	3	5	1	2	9	6	11
	MASE (Raw)	0.949	0.609	1.228	0.905	0.617	0.963	1.014	1.403	0.992	1.031	1.968	1.330
	CRPS (Raw)	0.029	0.019	0.038	0.028	0.020	0.032	0.031	0.046	0.030	0.032	0.061	0.042
Commodity Production	MASE (Norm.)	0.971	0.623	1.257	0.926	0.631	0.985	1.038	1.435	1.015	1.055	2.014	1.361
	CRPS (Norm.)	0.898	0.599	1.180	0.882	0.621	0.996	0.987	1.451	0.957	1	1.922	1.307
	MASE (Rank)	4	1	10	3	2	5	8	12	7	9	13	11
	CRPS (Rank)	4	1	10	3	2	7	6	12	5	9	13	11
	MASE (Raw)	0.914	0.905	0.928	0.950	0.914	0.912	0.949	1.205	0.794	0.939	0.960	1.027
	CRPS (Raw)	0.124	0.124	0.123	0.128	0.124	0.128	0.128	0.151	0.109	0.124	0.128	0.138
Commodity Import	MASE (Norm.)	0.734	0.726	0.744	0.763	0.734	0.732	0.761	0.967	0.637	0.753	0.771	0.824
	CRPS (Norm.)	0.698	0.695	0.693	0.717	0.699	0.720	0.721	0.851	0.613	0.699	0.720	0.776
	MASE (Rank)	5	2	6	9	4	3	8	12	1	7	10	11
	CRPS (Rank)	4	3	2	7	6	8	10	12	1	5	9	11
	MASE (Raw)	1.567	1.475	1.554	1.453	1.507	1.484	1.499	1.813	1.678	1.534	1.642	1.751
	CRPS (Raw)	0.214	0.237	0.213	0.190	0.223	0.195	0.201	0.199	0.185	0.214	0.221	0.197
WUI-Global	MASE (Norm.)	0.839	0.790	0.832	0.778	0.807	0.795	0.803	0.971	0.899	0.822	0.880	0.938
	CRPS (Norm.)	0.643	0.712	0.641	0.571	0.672	0.587	0.603	0.598	0.555	0.644	0.663	0.591
	MASE (Rank)	8	2	7	1	5	3	4	12	10	6	9	11
	CRPS (Rank)	8	12	7	2	11	3	6	5	1	9	10	4
	MASE (Raw)	0.961	0.946	0.976	0.971	1.005	0.970	0.975	1.022	0.971	0.992	0.959	0.963
	CRPS (Raw)	0.513	0.534	0.533	0.531	0.541	0.541	0.553	0.573	0.564	0.547	0.525	0.513
Global Price	MASE (Norm.)	0.718	0.706	0.729	0.725	0.751	0.725	0.728	0.763	0.725	0.741	0.716	0.719
	CRPS (Norm.)	0.623	0.647	0.646	0.644	0.656	0.656	0.671	0.695	0.683	0.664	0.636	0.623
	MASE (Rank)	3	1	9	7	11	5	8	12	6	10	2	4
	CRPS (Rank)	2	6	5	4	8	7	10	12	11	9	3	1
	MASE (Raw)	1.416	1.430	1.512	1.478	1.555	1.495	1.412	1.748	1.497	1.567	1.464	1.482
	CRPS (Raw)	0.132	0.133	0.141	0.140	0.144	0.145	0.131	0.172	0.148	0.146	0.139	0.136
Vehicle Sales	MASE (Norm.)	0.777	0.784	0.829	0.810	0.853	0.820	0.774	0.958	0.821	0.859	0.803	0.812
	CRPS (Norm.)	0.735	0.744	0.788	0.779	0.805	0.809	0.732	0.957	0.825	0.813	0.772	0.759
	MASE (Rank)	2	3	9	5	10	7	1	12	8	11	4	6
	CRPS (Rank)	2	3	7	6	8	9	1	12	11	10	5	4
	MASE (Raw)	0.861	0.835	0.937	0.759	1.311	0.791	0.750	0.903	0.882	0.773	0.786	0.865
	CRPS (Raw)	0.070	0.066	0.073	0.065	0.122	0.067	0.064	0.072	0.068	0.065	0.070	0.075
Online Retail II	MASE (Norm.)	0.611	0.592	0.664	0.538	0.930	0.561	0.532	0.640	0.626	0.548	0.557	0.614
	CRPS (Norm.)	0.610	0.571	0.640	0.570	1.062	0.581	0.559	0.630	0.594	0.566	0.612	0.652
	MASE (Rank)	7	6	11	2	12	5	1	10	9	3	4	8
	CRPS (Rank)	7	4	10	3	13	5	1	9	6	2	8	11
	MASE (Raw)	0.590	0.609	0.652	0.630	0.733	0.639	0.700	0.765	0.643	0.620	0.671	0.653
	CRPS (Raw)	0.234	0.242	0.255	0.247	0.272	0.254	0.274	0.302	0.253	0.248	0.268	0.258
Supply Chain-Customer	MASE (Norm.)	0.276	0.284	0.305	0.294	0.343	0.298	0.327	0.357	0.300	0.290	0.313	0.305
	CRPS (Norm.)	0.234	0.242	0.255	0.247	0.272	0.254	0.274	0.302	0.253	0.248	0.268	0.258
	MASE (Rank)	1	2	7	4	11	5	10	12	6	3	9	8
	CRPS (Rank)	1	2	7	3	10	6	11	12	5	4	9	8
	MASE (Raw)	0.581	0.554	0.614	0.598	0.636	0.615	0.669	0.666	0.613	0.611	0.661	0.661
	CRPS (Raw)	0.275	0.259	0.293	0.276	0.300	0.284	0.311	0.326	0.283	0.292	0.304	0.308
Supply Chain-Location	MASE (Norm.)	0.343	0.327	0.363	0.353	0.375	0.363	0.395	0.393	0.362	0.362	0.390	0.390
	CRPS (Norm.)	0.258	0.242	0.274	0.258	0.281	0.265	0.291	0.305	0.265	0.273	0.284	0.288
	MASE (Rank)	2	1	6	3	8	7	12	11	4	5	9	10
	CRPS (Rank)	2	1	7	3	8	5	11	12	4	6	9	10
	MASE (Raw)	0.627	0.605	0.650	0.649	0.668	0.659	0.699	0.705	0.649	0.650	0.683	0.694
	CRPS (Raw)	0.289	0.271	0.305	0.290	0.309	0.295	0.319	0.337	0.291	0.304	0.309	0.318
Supply Chain-Location	MASE (Norm.)	0.393	0.379	0.407	0.406	0.418	0.413	0.438	0.441	0.406	0.407	0.428	0.434
	CRPS (Norm.)	0.273	0.257	0.288	0.274	0.292	0.279	0.302	0.319	0.275	0.287	0.293	0.300
	MASE (Rank)	2	1	5	4	8	7	11	12	3	6	9	10
	CRPS (Rank)	2	1	7	3	8	5	11	12	4	6	9	10
	MASE (Raw)	0.731	0.716	0.834	0.758	0.899	0.763	0.741	0.776	0.767	0.807	0.869	0.817

Table 6. Full results of Per Dataset (Continued).

Dataset	Metric	TimesFM 2.5	Chronos2	Kairos	Moirai 2.0	VisionTS++	TiRex	Toto	Sundial	TimesFM 2.0	Chronos-bolt	Moirai	TimesFM 1.0
Azure2019-I	CRPS (Raw)	0.144	0.139	0.194	0.152	0.184	0.154	0.145	0.166	0.161	0.164	0.175	0.182
	MASE (Norm.)	0.668	0.654	0.762	0.693	0.822	0.697	0.677	0.709	0.701	0.738	0.795	0.747
	CRPS (Norm.)	0.492	0.473	0.662	0.518	0.630	0.528	0.494	0.568	0.550	0.561	0.599	0.621
	MASE (Rank)	2	1	10	4	12	5	3	7	6	8	11	9
	CRPS (Rank)	2	1	12	4	11	5	3	8	6	7	9	10
	MASE (Raw)	0.698	0.677	0.788	0.726	0.793	0.728	0.702	0.761	0.782	0.789	0.917	1.127
Azure2019-U	CRPS (Raw)	0.129	0.123	0.153	0.133	0.145	0.133	0.128	0.146	0.146	0.146	0.150	0.184
	MASE (Norm.)	0.690	0.669	0.779	0.718	0.784	0.719	0.694	0.753	0.773	0.780	0.906	1.114
	CRPS (Norm.)	0.565	0.538	0.673	0.584	0.637	0.585	0.563	0.639	0.641	0.640	0.658	0.805
	MASE (Rank)	2	1	8	4	10	5	3	6	7	9	11	13
	CRPS (Rank)	3	1	11	4	6	5	2	7	9	8	10	12
	MASE (Raw)	0.693	0.661	0.763	0.677	0.849	0.699	0.684	0.783	0.721	0.773	0.900	0.852
Smart Manufacturing	CRPS (Raw)	0.161	0.147	0.187	0.148	0.199	0.150	0.153	0.168	0.163	0.179	0.189	0.182
	MASE (Norm.)	0.602	0.574	0.662	0.588	0.737	0.607	0.594	0.680	0.626	0.671	0.781	0.740
	CRPS (Norm.)	0.283	0.257	0.328	0.260	0.349	0.264	0.269	0.295	0.286	0.314	0.331	0.320
	MASE (Rank)	4	1	7	2	10	5	3	9	6	8	12	11
	CRPS (Rank)	5	1	10	2	12	3	4	7	6	8	11	9
	MASE (Raw)	0.713	0.712	0.713	0.714	0.716	0.719	0.720	0.734	0.717	0.715	0.728	0.717
MetroPT-3	CRPS (Raw)	0.167	0.166	0.175	0.167	0.167	0.167	0.169	0.188	0.178	0.173	0.172	0.180
	MASE (Norm.)	0.685	0.685	0.685	0.686	0.688	0.691	0.692	0.706	0.689	0.687	0.700	0.689
	CRPS (Norm.)	0.610	0.610	0.641	0.613	0.612	0.614	0.618	0.689	0.653	0.632	0.629	0.657
	MASE (Rank)	2	1.667	3.333	3.667	6.667	9	9.333	11.667	6.667	5.333	11.333	7.333
	CRPS (Rank)	3	1.667	7.333	4	2.667	5.333	7	11.333	9.333	7	8.667	10.667
	MASE (Raw)	0.625	0.629	0.666	0.665	0.673	0.645	0.645	0.669	0.690	0.689	0.673	0.711
MetroPT-3	CRPS (Raw)	0.256	0.255	0.288	0.253	0.264	0.256	0.262	0.313	0.300	0.280	0.261	0.324
	MASE (Norm.)	0.740	0.745	0.788	0.787	0.797	0.763	0.764	0.792	0.817	0.815	0.797	0.842
	CRPS (Norm.)	0.677	0.674	0.762	0.670	0.698	0.679	0.693	0.829	0.790	0.742	0.691	0.854
	MASE (Rank)	1.667	1.667	7	7	8	3.667	4.333	7.333	9.667	9.333	7	11.333
	CRPS (Rank)	2	2.333	8.333	2.667	6.667	3.667	6	11	8.667	9	6.333	11.333

F. Visualization

Our platform features an interactive visualization tool for inspecting predictions across different test windows. Key functionalities include zooming and the display of probabilistic quantiles to assess forecast confidence. The visualization employs a distinct color schema for clarity: the blue region indicates the training history, the yellow region marks the overall test set, and the red region highlights the specific target window currently under evaluation. The following predictions are all from TimesFM 2.5.

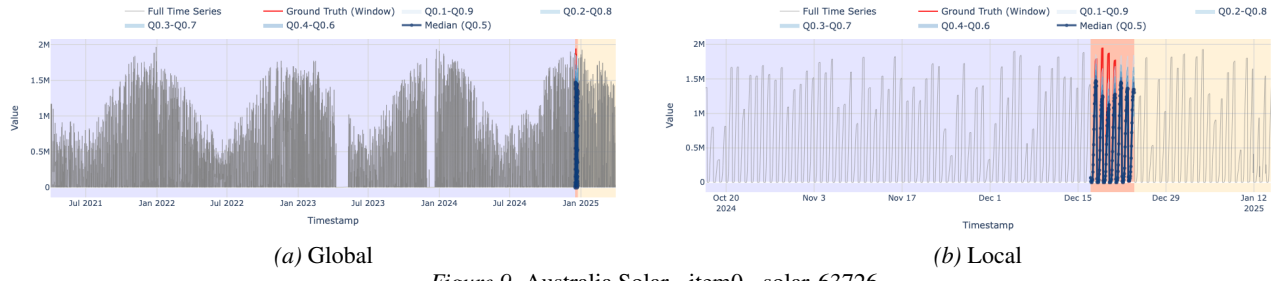


Figure 9. Australia Solar - item0 - solar_63726

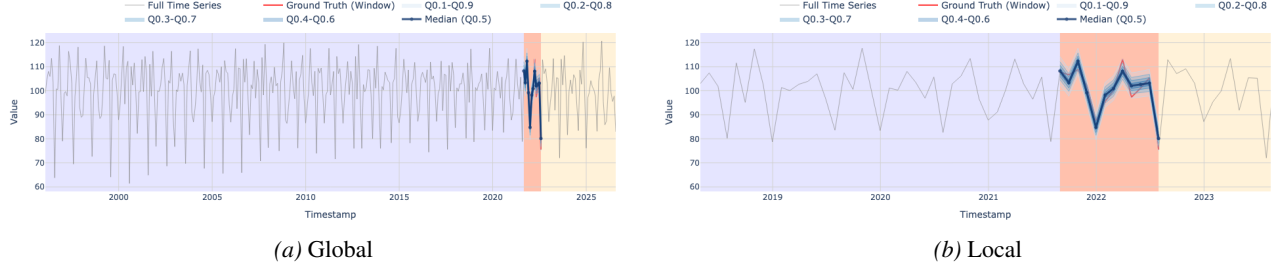
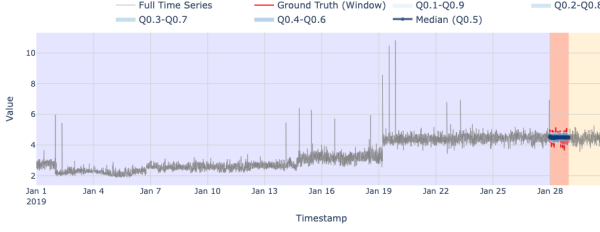
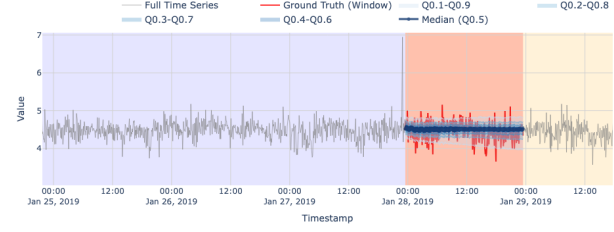


Figure 10. Auto Production SF - RSF AutoProduction

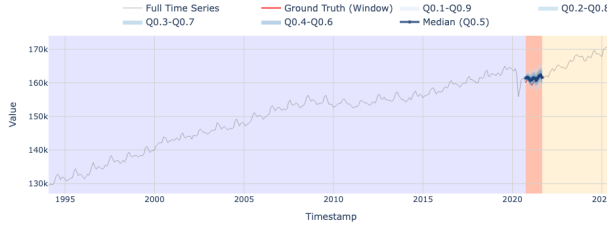


(a) Global



(b) Local

Figure 11. azure2019 I - item_1 - min.cpu

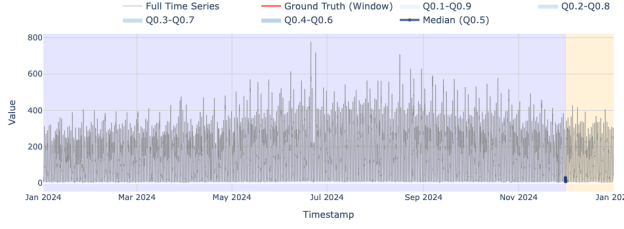


(a) Global



(b) Local

Figure 12. US Labor - item0 - CivilianLaborForceLevel

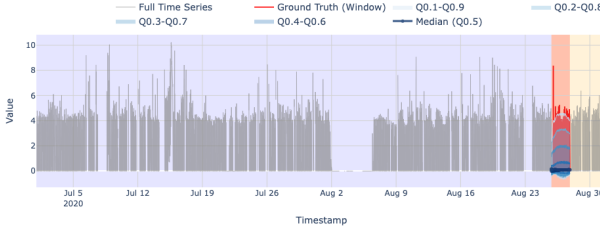


(a) Global

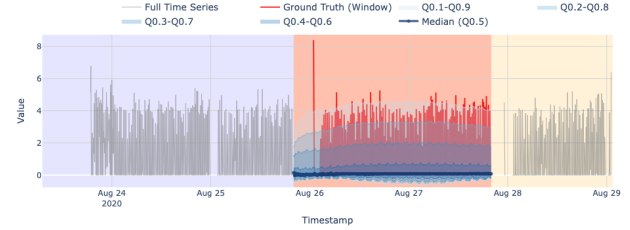


(b) Local

Figure 13. Finland Traffic - volume



(a) Global



(b) Local

Figure 14. MetroPT-3 - item0 - TP2

G. Limitations and Future Directions

Pattern Granularity and Data Sparsity. In our current pattern-level evaluation, we employ a median-based binary threshold to categorize feature strengths. While we explored finer-grained quantization (e.g., dividing features into 5 quintiles, representing 5 levels from Strong to Weak), we encountered a combinatorial explosion challenge: the number of subgroups grows exponentially with the number of combined patterns. This leads to severe data sparsity in intersectional groups, rendering statistical analysis unreliable. Future work will address this by expanding the scale of variates in the benchmark and developing more sophisticated pattern retrieval mechanisms to enable fine-grained analysis without compromising statistical validity.

Task-Aligned Evaluation Metrics. Time series forecasting fundamentally serves downstream decision-making. However, standard general-purpose metrics like MASE and CRPS often fail to provide actionable insights specific to operational

contexts. For instance, in financial scenarios, the directional accuracy (i.e., predicting the correct rise or fall to guide trading actions) is often more critical than minimizing the absolute magnitude of error. Furthermore, general metrics are known to be sensitive to data processing factors such as scaling and aggregation schemes (Brigato et al., 2026). As a task-centric benchmark, our next phase aims to align evaluation protocols with specific downstream requirements, moving beyond generic error minimization to provide metrics that reflect the true actionable utility of the forecasts in real-world applications.